The Thesis committee for Nhut Minh Nguyen

Certifies that this is the approved version of the following thesis:

SYSTEMATIC STUDY OF FOAM FOR IMPROVING SWEEP EFFICIENCY IN CHEMICAL ENHANCED OIL RECOVERY

APPROVED BY SUPERVISING COMMITTEE:

Supervisor: _____

Quoc P. Nguyen

_____

Gary A. Pope

SYSTEMATIC STUDY OF FOAM FOR IMPROVING SWEEP EFFICIENCY IN CHEMICAL ENHANCED OIL RECOVERY

by

Nhut Minh Nguyen, B.E.

Thesis

Presented to the Faculty of the Graduate School
of the University of Texas at Austin
in Partial Fulfillment
of the Requirements
for the Degree of

Master of Science in Engineering

The University of Texas at Austin

December 2010

Dedication

To my parents, Lan and Rang, and my beloved Thanh Mai.

ACKNOWLEDGEMENTS

Endless thanks must go to my supervisor, Dr. Quoc P. Nguyen, for the valuable knowledge, unconditional guidance and encouragement he has given to me. Without his enormous motivation and sharing, this journey would have been much more difficult to accomplish. To be honest, supervising a non-experienced, restive and perhaps, reactive student like me is very difficult. But Dr. Nguyen with his extraordinary patience and benevolence went through all of that and guided me to the success of my learning and development in petroleum graduate program at The University of Texas at Austin. Once again, immeasurable amount of thanks goes to Dr. Nguyen for not only being an understanding supervisor, but also a mentor, and a friend. Special appreciations also go to Dr. Gary A. Pope. He always found time to answer my questions no matter how busy he was. His shear expertise in the field of chemical EOR has helped to improve my knowledge.

Many thanks must be sent to Mr. Glen Baum, Mr. Tony Bermudez, and Mr. Gary Miscoe for their constant help on setting up experimental facilities, familiarizing with new tools and keeping the lab in clean and safe conditions. Special thanks to Dr. Sujeewa for enormous help on providing essential materials as well as material procurement.

Last but not least, deepest thanks to my parents for bringing me to this life and sacrificing everything for my success. I must give the deepest love to my lovely girlfriend, Thanh Mai, for keeping me in her heart all the times and giving me the strength for not to give up.

December 2010

Abstract

SYSTEMATIC STUDY OF FOAM FOR IMPROVING SWEEP EFFICIENCY IN CHEMICAL ENHANCED OIL RECOVERY

Nhut Minh Nguyen, M.S.E

The University of Texas at Austin, 2010

Supervisor: Quoc P. Nguyen

Foam-assisted low interfacial tension and foam-improved sweep efficiency are attractive enhanced oil recovery (EOR) methods with numerous studies and researches have been conducted in the past few decades. For example, CO_2-Enhanced Oil Recovery (CO_2-EOR) is very efficient in terms of oil displacement. However, due to the low viscosity of super critical CO_2, the process usually suffers from poor sweep efficiency. One method of increasing sweep efficiency in CO2-EOR has been identified through the use of surfactants to create "foams" or more correctly CO_2-in-water (C/W) macroemulsions.

Polymer flooding techniques such as Alkali – Polymer (AP), Surfactant – Polymer (SP), and Alkali – Surfactant – Polymer (ASP) have been the only proven chemical EOR method in sandstone reservoirs with many successful pilot tests and field projects. However, the use of polymer is limited in carbonates due to unfavorable conditions related to natural characteristics of this type of lithology. In this case, foam-assisted EOR, specifically Alkali – Surfactant – Gas (ASG) process, can be an alternative for polymer flooding. It is a fact that large amount of the world's oil reserves resides in carbonate reservoirs. Therefore, an increase in oil recovery from carbonates would help meet the world's increasing energy demand.

This study consists of twp parts: (1) the development of new surfactant for creating CO_2 – in – water macroemulsions for improving sweep efficiency in CO_2 – EOR processes; (2) systematic study of ASG method as a novel EOR technique and an alternative for polymer flooding in carbonate reservoirs. Both studies are related to the use of foam as a mobility control agent.

In the first part, the design and synthesis of twin tailed surfactants for use at the CO_2/water interface is discussed. The hydrohobes for these surfactants are synthesized from epichlorohydrin and an excess alcohol. Subsequent ethoxylation of the resulting symmetrical dialkyl glycerin yields the water soluble dual tailed surfactants. The general characteristics of these surfactants in water are described. A comparison is carried out between twin-tailed dioctylglycerine surfactants and linear secondary alcohol surfactant based on results from a core flood. The results show that even above the cloud point of the surfactants, the twin tailed surfactants create a significant mobility reduction, likely due to favorable partitioning into the CO_2 phase. The data covers surfactant structures designed specifically for the CO_2-water interface and can be used by producers and service companies in designing new CO_2-floods, especially in areas that might not have been considered due to problems with reservoir heterogeneity.

Second part contains a systematic study of ASG process on carbonate rocks through a series of experiments. The purpose is to demonstrate the performance as well as the potential of ASG as a new EOR technique. In this study, basic concepts in chemical EOR are presented, while the design of chemical formulation, phase behavior, and the role of foam are discussed in details. Experimental results showed relatively good recovery, low surfactant retention. However, pressure drop during chemical injections were high, which indicates the formation of both strong foam and viscous microemulsion at the displacement front when surfactant starts solubilizing oil. Overall, ASG showed good performance on carbonate rocks. Optimization can be made on surfactant formula to form less viscous microemulsion and therefore improve efficiency of the process.

TABLE OF CONTENTS

LIST OF TABLES

LIST OF FIGURES

CHAPTER 1

INTRODUCTION

1.1 OVERVIEW

1.1.1 CO_2 – Enhanced oil recovery (CO_2 – EOR)

It was reported that about 129 CO_2 EOR projects being conducted around the world, and amazingly only 15 were outside of the US. In the US, CO_2-EOR currently accounts for ~3-4% of total US oil production and is expected to grow to more than 20% by 2030, mainly due to the development of CO_2 resources and the building of subsidized pipeline infrastructure in the 1980s (ARI,2010). Although the US is leading in the area of EOR production, it has been suggested that CO_2 EOR could have added as much as 46 BBbls of oil production in the Middle East if suitable sources of CO_2 were made available (ARI and Melzer 2009).

When compressed at typical reservoir pressures, CO_2 has the benefit of becoming a supercritical fluid and is almost miscible with light to medium crude oil. For the purpose of clarity, unless otherwise stated, all references to CO_2 in Chapter 3 refer to supercritical CO_2. The displacement efficiency of a miscible CO_2 flood can often exceed 90%, however, due to the low viscosity and subsequent mobility mismatch of the supercritical fluid with the oil, the sweep efficiency is generally half that of a corresponding water flood. The typical solution to a mobility based sweep efficiency problem is to increase the viscosity, by either adding a viscosifying agent (typically a polymer) or by forming an emulsion or foam with a second phase (gas foams or emulsions). The use of foam for mobility control in CO_2-EOR was first proposed in the 1960s and has since been validated in several pilot studi1es which have been reviewed (Fischer and Holm 1978 and Turta and Singhal 1998).

In this study, the author refers to emulsions of super critical CO_2 and water as foams. Although, the term emulsion might be more scientifically appropriate, the term foam has become so dominant in the literature in respect to CO_2-EOR and therefore the author has chosen to follow the wide-accepted terminology.

Although foam can be used in many different ways in the oilfield, this study will focus on general mobility and conformance control in a reservoir with high permeability contrast. The idea is to generate a bank of foam that can propagate in to the formation and not simply modify the injectivity in the near wellbore region.

1.1.2 Alkali – Surfactant – Gas process (ASG)

Within the past few decades, polymer flooding techniques such as Alkali – Polymer (AP), Surfactant – Polymer (SP), and Alkali – Surfactant – Polymer (ASP) have been the only proven chemical EOR method in sandstone reservoirs with many successful pilot tests and field projects. However, the use of polymer is limited in the other lithology, carbonate reservoirs, due to:

- The viscosity increasing feature of polymer lies in its high molecular weight. In tight reservoirs such as carbonates, this feature may cause plug-up or result in very high pressure gradient. Smaller polymer molecular weight can be used in this case but the costs will be increased and eventually becomes uneconomic.
- Permeability reduction was believed as an advantage of polymer flooding since reduction in polymer mobility was reported to be greater than expected based on solution viscosity. Unfortunately, reservoir permeability is generally decreased with increasing permeability reduction, resulting in poor injectivity and diminishing sweep efficiency.
- Polymer properties can be destabilized at high temperature. For instant, Partially Hydrolyzed Polyarcylamide (HPAM), the most common commercial polymer used for polymer flooding, loses its viscosity when undergoes thermal oxidation at 60^0C and above (Niu *et al*., 2001).
- Polymer viscosity is very sensitive to salinity. Lake (1989) showed that, as a thump of rule, the viscosity of polymer solution decreases by a factor of 10 with 10 times increase in sodium chloride (NaCl) concentration. Moreover, HPAM polymers and HPAM derivatives even more sensitive to hardness. This limits the use of polymer for high salinity applications.

- There may be some unexpected interactions between polymer and surfactant under certain reservoir conditions.

Foam enhanced oil recovery, specifically Alkali – Surfactant – Gas (ASG) can be an alternative method to polymer flooding in conditions which are not feasible for the use of polymer. The concept of using foam for mobility control was first introduced by Lawson and Reisberg in 1980. At that time, foam enhanced oil recovery process was not quite immediately accepted and considered applicable due to limitations of technique and understanding of process mechanisms. However, there have been many field tests of foam application since then, as the understanding of foam mobility control was advanced. For example, foam was used for surfactant aquifer remediation at Hill AFB in Utah (Hirasaki 1997, 2000), alkaline surfactant flooding in China (Zhang 2000; Wang 2001), or the most successful field pilot test of foam mobility control in Snorre field (Blaker 2002).

Foam can be generated by co-injection or alternate injection of gas and surfactant slug. The use of foam as a means of reducing gas mobility can improve the efficiency of gas EOR in three ways:

- Diminish viscous fingering and gravity segregation by creating more resistance to gas flow since gas bubbles are surrounded in foam by thin films of liquid called lamella. A portion of gas is trapped by lamella and becomes immobilized, resulting in reduction of gas relative permeability. Thus lower gas mobility and improve sweep efficiency of the process.
- The addition of surfactant in aqueous phase reduces capillary forces by lowering interfacial intension between displacing fluids and trapped oil.
- Foams can collapse in low permeability regions if capillary forces are sufficiently high enough to drain the liquid in thin films surrounding gas bubbles (Schramm *et al.,* 1994). This ability, if happens under certain circumstances, will allow solution of gas/water/surfactant to travel deeper into low permeability zones where polymer solution can not reach (Smith *et al.,* 1988).

In Alkali – Surfactant – Gas (ASG) process, the level of foam stability determines the mobility reduction magnitude of gas and surfactant slug. Weak or unstable foam leads to unfavorable mobilities of gas and surfactant solution and thus poor displacement efficiency, whereas stable foam lowers mobilities of tow phases to a favorable value and improves displacement efficiency of the process. Therefore, one of the most important understandings about foam performance is how to generate and sustain a flowing of "strong" or "stable" foam. Rossen (1988) reported a minimum pressure gradient needed to initiate and sustain a foam flow in porous media. If this minimum pressure can not be sustained from injection well to producer, foam will stop flowing and cause plugging in the zone.

Another important understanding is the foundation of a foam flow regime in which pressure gradient is a function of only liquid rate. In this regime, gas mobility increases with increasing gas fractional flow and decreasing permeability. This foundation makes foam extremely useful in layered reservoirs for improving sweep efficiency (Bertin 1998; Kovscek 2002).

Recognizing the potential of ASG process, this thesis was conducted with intention to partially fulfill the lack of study on this EOR technique. Since polymer flooding is the most dominant EOR method in sandstone, the use of foam as mobility control agent may widen the application of chemical EOR technique to other types of lithology. This extension will ensure the supply for growing demand in economical energy while the remaining of reserves are quickly being drained and number of new discoveries has been declining steadily in the last few decades.

1.2 RESEARCH OBJECTIVES

This research was performed to serve these following objectives:

- Develop a new class of twin tailed surfactant based on glycerin and designed for the supercritical (sc)CO_2 – water interface.
- Demonstrate the potential of Alkali – Surfactant – Gas as a novel EOR technique in carbonate reservoirs.

1.3 ORGANIZATION OF CHAPTERS

In Chapter 2, a literature review of foam properties and previous works on foam study is presented. Secondly, a brief introduction to CO_2 – foam in EOR takes place. Finally, description of chemical flooding in general and Alkali – Surfactant – Gas process is carried out.

Chapter 3 contains the work of developing new class of surfactant for supercritical CO_2 – water interface. Experiment descriptions and results discussion are presented.

Chapter 4 demonstrates the performance of ASG on carbonate rocks. Experiment procedure, phase behavior, experimental results, as well as the potential of ASG process are discussed in this chapter.

Chapter 5 is an overall summary of the research and suggestions for future work.

CHAPTER 2

LITERATURE REVIEW

This chapter provides fundamental background and previous study on foam application. Not all topics related to foam is covered in this chapter. Instead, a brief overview of important topics is presented to help the readers understand the following chapters of this research. Followed are an introduction to CO_2 – foam in EOR and brief description chemical EOR process.

2.1 BASIC CONCEPTS OF FOAM

2.1.1 Definition

Foam is commonly defined as a dispersion of gas bubbles in aqueous phase. The dispersed phase (gas) is preferred as discontinuous phase or sometimes internal phase, whereas liquid phase is continuous or external phase (Hirasaki, 1989). The contact between gas bubbles in liquid occur through various thin liquid films called "lamella" (plural "lamellae"), usually containing surfactants to strengthen the stability of these films (Figure 2.1). In the absence of oil, lamella governs foam stability. If this film is stable, foam is stable and vise versa. The stability of lamellae can be improved by adding surfactant in aqueous phase.

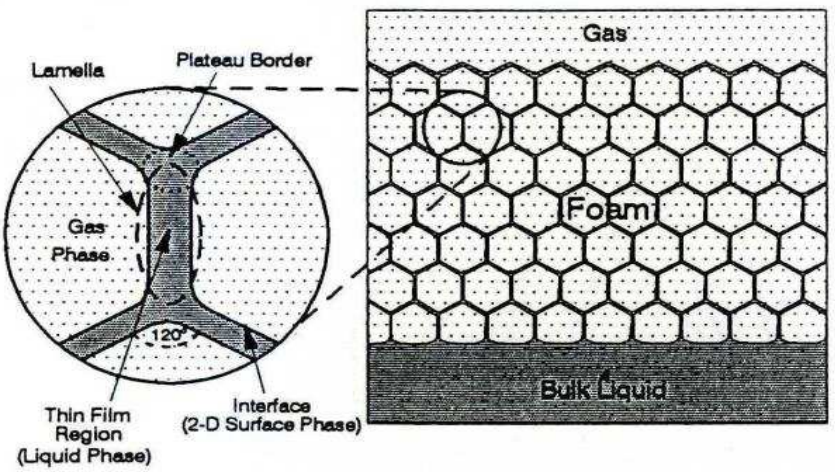

Figure 2.1 – Generalized foam system (Schramm, 1994)

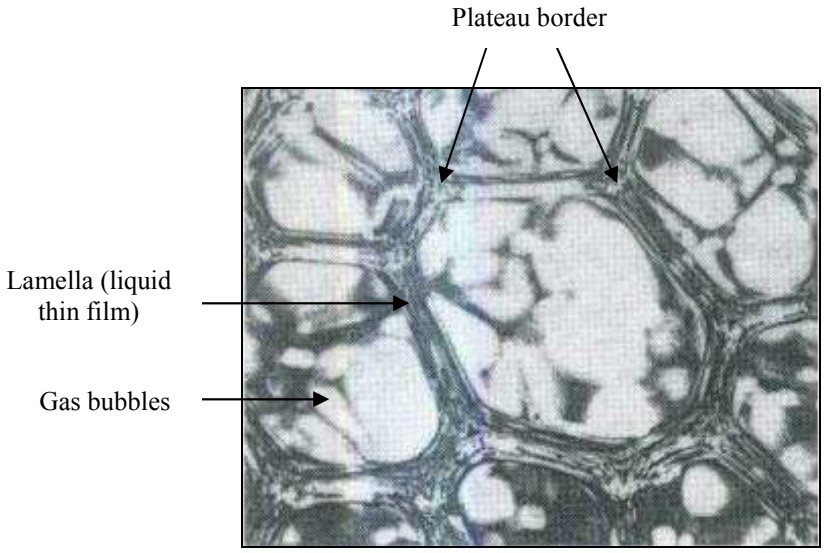

Figure 2.2 – A picture of foam system (Exerowa, 1993)

2.1.2 Classification of Foam

Generally, foam can be divided into two main groups: bulk foams and foams in porous media.

2.1.2.1 Bulk Foam

Bulk foam refers to the volume in which foam resides is much larger than individual bubbles (Rossen, 1993). Bulk foam can be treated a single homogeneous phase where the velocities of gas and liquid phases are considered similar since bubbles in bulk foam are relatively small compared to flow channel (Calvert, 1989). In oil industry, bulk foam is used in drilling, cementing and fracturing. The half-life time of bulk foam is sometimes used to evaluate the forming ability of surfactants.

2.1.2.2 Foam in Porous Media

In contrast, foam in porous media is characterized by the distribution of pore size and pore throat (Yan, 2006). According to Ettinger and Radke (1992), an individual bubble occupies one or several pore bodies in porous media, meaning that foam does not behave as a continuous and homogeneous phase within porous media. Precisely speaking, foam in porous media is a discontinuous phase in which gas

bubbles are separated from each other by liquid thin films. To avoid any confusion that might happen, from this point to the rest of this thesis the word “foam” refers to foam in porous media.

Having the flow of foam in porous media results in gas trapping or gas flowing as a continuous or discontinuous phase. Trapped gas occurs when foam completely blocks all gas-flow paths. Continuous gas-flow results the existence of some flow-channels that are not interrupted by lamellae. On the other hand, in discontinuous gas-flow, all channels are interrupted by lamellae and foam flows as connected bubbles trains (Figure 2.3).

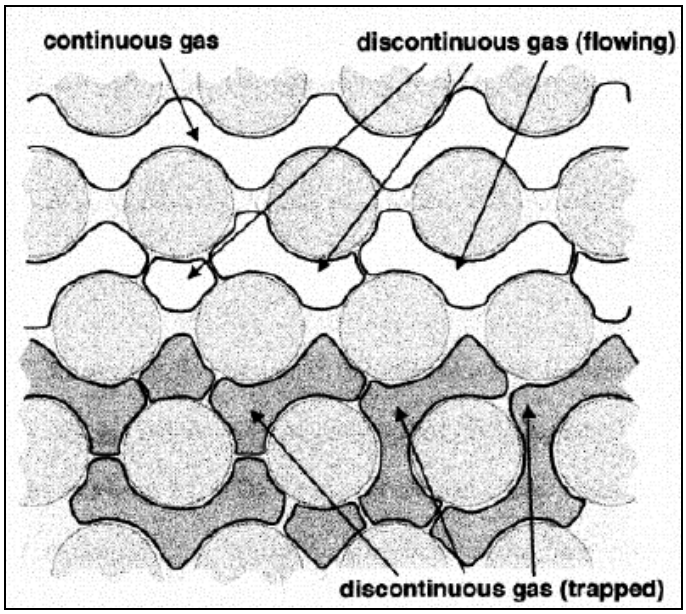

Figure 2.3 – Schematic of gas flow in porous media in the presence of foam (Tanzil, 2001)

2.1.3 Foam Properties

2.1.3.1 Quality

Foam quality represents the volume of gas contained in foam. This property is usually expressed as percentage or fraction, and defined as:

$$\text{Foam quality (\%)} = \frac{\text{gas volume}}{\text{gas volume + liquid volume}} \times 100$$

In coreflood experiment, foam quality is expressed as:

$$\text{Foam quality (\%)} = \frac{\text{injection gas rate}}{\text{injection gas rate + injection rate}} \times 100$$

where injection gas rate is calculated at core conditions (elevated pressure) since gas volume changes with pressure and temperature, leading to foam quality is a function of pressure and temperature, together with foam constituents.

The equation above suggests a wide range for foam quality. However, foam must be used within certain range in which it exhibits the mobility reduction characteristics. Chang *et al* (1999) and later Hutchins (2005) conducted experiments and estimated that range to be from 40% to 95% of foam quality.

Other researchers have tried to relate the foam quality to foam viscosity. Mitchell (1970) found that below quality of 55% foam behaves like a Newtonian fluid, where viscosity is independent of shear-stress, and above 55% foam becomes non-Newtonian with shear-thinning properties. Bullen *et al* (1975) stated that mobility reduction can not be accomplished at low (<40%) or extreme high quality (>95%) since foams are unstable at these conditions.

2.1.3.2 Texture

Of equal importance to foam quality is foam texture, i.e. bubble size and bubble size distribution. It has been well-known that bubble size is one of parameters influencing stability of foam, specifically, foam is more stable with narrow bubble size distribution (40-90 μm) compared to wide size distribution (28-205 μm) (Friedman and Jensen, 1986). Nguyen *et al.,* (2004) also proposed that stable fine-textured foam exhibits low mobility resulting from both reduced gas permeability and effective viscosity.

Foam texture can also be described in terms of average bubble radius (or diameter) or a distribution of radii (Stenuf *et al*, 1953). The texture defines how foams

flow through a porous media. If average bubble diameter is much smaller than that of the pores, foams flow as dispersed bubbles in pore channels. In the opposite case where average bubble size is much larger than pore diameter, foams flow as progression of films separating individual bubbles (Lake, 1989) and can be trapped in small pore channels where low capillary pressure or pressure gradient occurs. Figure 2.4 shows typical bubble size distribution, obtained from David and Marsden, 1969.

In general, foam texture depends on type and concentration of surfactants, pore geometry, pressure and foam quality. For example, an increase in concentration of surfactant leads to the decrease in bubble size.

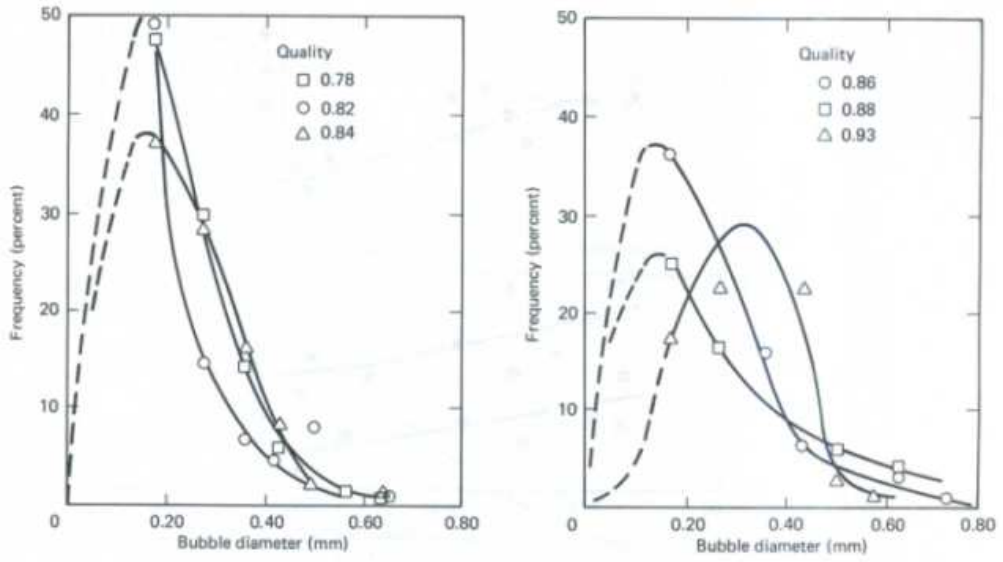

Figure 2.4 – Bubble size distribution (David and Marsden, 1969)

2.1.3.3 Rheology

Foams have an extreme variability in flow properties. Some foams flow just like ordinary fluids while the others are likely stiff and elastic. Several researchers have considered foam as fluids or as microscopically uniform bodies to study the rheology because of that characteristic.

All results and data of foam rheology studies up to date suggest that foams are frequently pseudoplastic, which means foam has shear-dependent viscosity, or shear-

thinning properties. Thus true foam viscosity can not be measured. Instead, apparent viscosities are calculated through measured shear stresses obtained at different shear rates. Results have shown that foam apparent viscosity decreases with increasing shear-rate and with decreasing foam quality (Marsden, 1964). However, Sharma (1965) reported that on microscopic level foams may be flowing as bubble trains much smaller than the pores, or as a series of foam membranes of changing sizes, shapes and configurations. In this case, apparent viscosity does not apply, but Darcy's law can be used to calculate foam mobility, that is, the ratio of effective permeability to viscosity.

Many efforts have been made for better understanding of foam rheology. Van Wazer (1963), Fredrickson (1964), and later Whorlow (1980) proposed very useful experimental techniques and if performed with care and precision, these techniques can be applied to measuring foam shear stress. However, conducting such an experiment has experienced many difficulties, making the measurements irreproducible and not representative of original foams (Schramm, 1994).

2.1.4 Foam Generation

Speaking of pore-level, there are three fundamental mechanisms in which foam is generated: snap – off, leave – behind, and lamellae division. Understanding of these mechanisms is essential to derive physically meaningful rate expressions for foam generation and coalescence.

2.1.4.1 Snap –Off

This is s very important mechanism for bubble generation in porous media. Roof (1970) was the first who indentified and explained this phenomenon to understand the origin of residual oil. Snap – off repeatedly occurs during multiphase flow in porous media regardless of the presence or absence of surfactant. In the presence of surfactant, three types of snap – off exist, depending upon local liquid saturation and the pore-body to pore-throat aspect ratio (Chambers and Radke, 1991).

Pre-neck snap – off occurs when a given pore throat is blocked at the upstream by a bubble. Depending on the geometry of pore throat, snap – off ensues

when there is an adequate amount of liquid just upstream accumulates and squeezes the initial bubble to smaller one.

Rectilinear snap – off preferentially exists further downstream in long pores with sharp corners (Chambers and Radke, 1990).

Neck snap – off (or Roof snap – off) as illustrated in Figure 2.4. A bubble first approaches and blocks a pore throat at the upstream. At this point, capillary pressure rises and must exceed the entry pressure to let the bubble go through the pore throat. Upon entering the downstream body, the capillary pressure at bubble front falls with expansion at the interface. This negative gradient in capillary pressure initiates a gradient in liquid pressure that drives the liquid from the pore body into the pore throat where it accumulates as a collar. Roof (1970) found that a pore must have a body-to-throat size aspect ratio of at least two in order to produce a sufficient pressure gradient of wetting phase for this mechanism to happen.

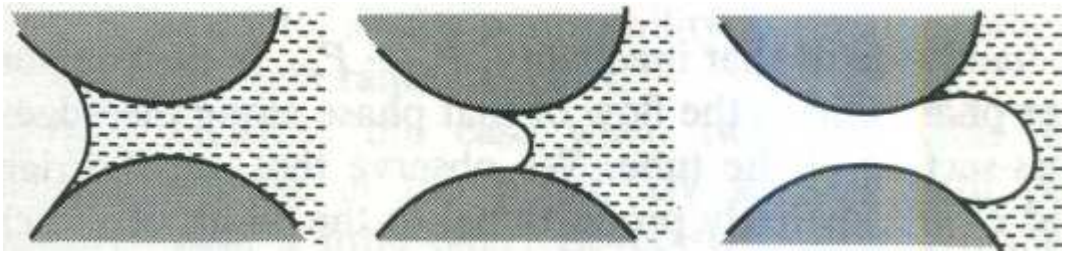

Figure 2.5 – Schematic of Neck snap – off mechanism (Charles, 1991)

2.1.4.2 Lamella Division

This mechanism contains the breaking-up of a bubble into two smaller ones when stretching around a branch point of a flow channel (Nguyen *et al.*, 2004) as displayed in Figure 2.5. Thus, mobile foam bubbles must be pre-existed.

Figure 2.6 – Schematic of lamella division mechanism (Nguyen *et al.*, 2004)

There division of a lamella is controlled by several factors. First is the size of a bubble. Chambers (1990) has found that foam bubble does not divide when approaching a branch point if its size is smaller than that of the pore-body. At this point, one may say the division generally occurs if bubble size is larger than pore-body size. However, that statement has remained controversial since the lamella may be drained of liquid and coalesced in the process (Gauglitz, 1990). Second, there is a probability that bubble division depends on the occupancy of surrounding pores (Prieditis, 1988). Division occurs when there are no foam bubbles or lamellae surrounding branch point. On the other hand, the presence of stationary bubbles or lamellae significantly reduces the number of branch points and diverts the once branching flow down one path by acting as flexible pore walls. Therefore, division is prohibited.

2.1.4.3 Leave – Behind

As described in Figure 2.6, two gas menisci invade pore bodies. First, a lens is left behind as two menisci converge downstream and the lens may drain to a thin film (lamella) later (Owete and Brigham, 1987).

While lamellae created by both snap – off and lamella – division are generally perpendicular to local flow direction, leave – behind generates lamellae that are parallel to flow direction and thus do not make gas phase discontinuous. Ransohoff and Radke (1988) found that lamellae created by leave – behind gave a five-fold

reduction in gas permeability compared to several hundred fold reduction in gas mobility resulted from flow-perpendicular lamellae (Ettinger and Radke, 1992).

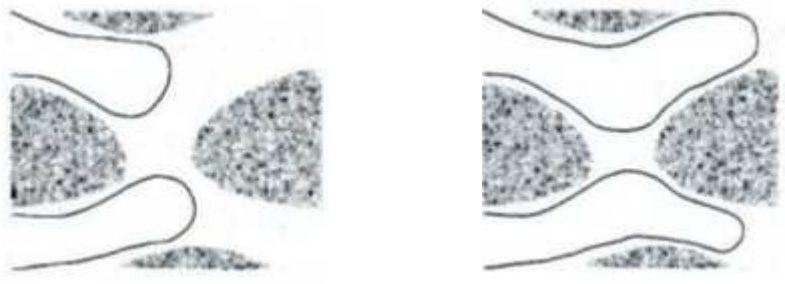

Figure 2.7 – Schematic of leave – behind mechanism (Nguyen *et al.*, 2004)

2.1.5 Effect of Foam on Gas and Liquid Mobilities

2.1.5.1 Gas Mobility

Gas mobility can be drastically reduced in the presence of foams in porous media. By definition, foam is a dispersion of gas bubbles in aqueous phase, separated by thin liquid films called lamella (plural lamellae). These lamellae can be stationary or in motion. Stationary lamellae trap the gas and make it immobilized (Friedman *et al.*, 1991), whereas moving lamellae cause a resistance to gas flow due to the surface tension on individual lamellae and drag forces acting on them when they slide along the pore bodies. Both cases result in lower gas mobility but with different mechanisms. In the first case, gas relative permeability is decreased with increasing gas saturation trapped by stationary lamellae. On the other hand, second case is likely to increasing gas apparent viscosity, not actual viscosity, since a portion of gas flow experiences the "flow-resistance" caused by moving lamellae. Therefore, effect of foam on gas mobility can be understood as an increase in gas apparent viscosity or as a decrease in gas relative permeability.

Bernard and Holm (1964) performed a study on mobility reduction of foams as a means of decreasing gas relative permeability. Experiments were conducted in a strategy that would enable the comparison of two main mechanisms on this reduction: (1) the increase in trapped gas, and (2) blocking of pore throats due to formation of

lamellae. From figure 2.8, the results indicate that gas permeability was reduced significantly since lamellae were stabilized in the presence of surfactant (the top and bottom curves). However, the middle curve does not show an increase in gas saturation due to trapping in both cases. This leaded to conclusion that the effect of increasing trapped gas saturation is not comparable to that of pore throat blocking.

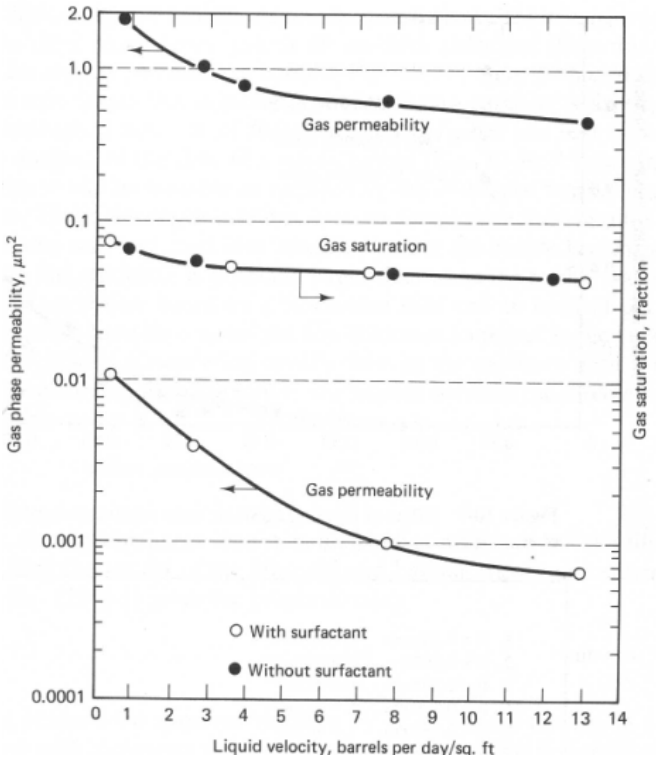

Figure 2.8 – Effect of liquid rate and gas saturation in gas permeability with and without surfactant (Bernard and Holm, 1964)

2.1.5.2 Liquid Mobility

Liquid mobility is said to be reduced by reducing relative permeability in the presence of foam. However, foam affects liquid relative permeability not by changing k_{rw} but by indirectly lowering liquid saturation S_w. Since total saturation of all phases remains unchanged, an increase in trapped gas saturation as discussed above results in a decrease in liquid saturation, which implies lower liquid relative permeability.

However, this explanation has remained controversial since experimental results showed opposite trend. For example, experimental data from Bernard *et al* (1965) indicated neither gas saturation nor the foaming agent have an effect on liquid relative permeability. In this case, liquid relative permeability increases with increasing liquid saturation (Figure 2.9).

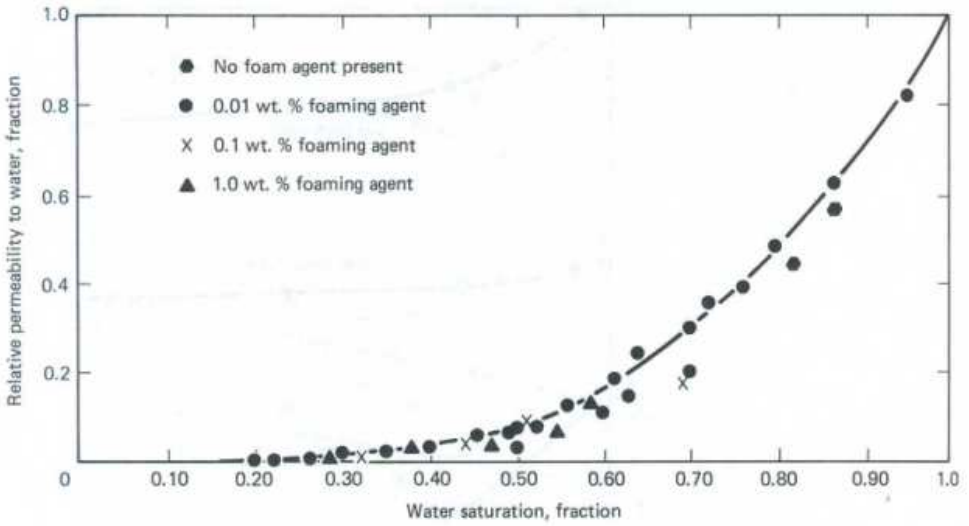

Figure 2.9 – Effect of foam on liquid relative permeability (Bernard *et al*., 1965)

2.1.6 Foam Stability

The mechanisms of foam stability can be understood based on a film approach, that is, the structure and stability of liquid films (lamellae). The more stable the lamellae, the more stable the foam. However, destruction of lamellae leads to foam coalescence. Well-known mechanism governing lamellae destruction can be listed here as: film drainage, gas diffusion, and oil effect. Moreover, some other factors that affect the lamella stability will also be discussed at the end of this section.

2.1.6.1 Film Drainage

This mechanism is the dominance in lamella destruction. In foam, gas bubbles are separated by liquid films (lamellae). These films will undergo a so-called thinning process in which eventually leads to the rupture or reaching to a metastable super-thin

state of these films (known as “black spot formation” because the films have black or grey color at this thickness). Foam coalescence is controlled by this process.

Two indicators of thinning process are *drainage time* and *critical thickness* of a lamella. First indicator implies the time when thinning of a lamella reaches critical thickness. Second indicator defines the thickness, below which the lamella starts to coalesce. These indicators have been proven to be a function of many parameters, such as viscosity, surface elasticity, ratio of gas to liquid viscosities, surface absorption and surfactant solubility (Rao, 1982; Wasan, 1987). A relationship between critical thickness and surfactant concentration is well-known, that is, an increase in surfactant concentration results in decreasing of critical thickness. However, the reverse of this relationship remains unclear in the case of a static lamella experiencing a stretching-contracting motion (Wasan, 1987).

Two main mechanisms governing film drainage are: gravity and capillary suction (at Plateau borders). *Gravity drainage* is usually observed in thick lamellae where foam is first created (Rossen, 2004). In foam, liquid is driven down by gravity force through connected liquid films. This mechanism was found to be decelerated with increasing the bulk viscosity of foaming solution or decreasing the liquid fraction of foam.

Capillary drainage due to capillary pressure (or suction at Plateau borders) is the main mechanism for film drainage in thin lamellae. Figure 2.10 represents pressure differences across curved surfaces in a foam lamella (from Schramm, 1994). As observed from this schematic, two curvatures at the center of lamella are almost parallel, whereas curvatures at Plateau borders are much more of a curve. Therefore, radius of curvature at center lamella R_{1A} is much larger than that at Plateau borders, R_{1B}. In foam, capillary pressure is defined as the difference between gas and liquid pressures, as below:

$$P_{CA} = P_G - P_A \quad (1)$$

$$P_{CB} = P_G - P_B \quad (2)$$

where P_{CA} : capillary pressure at center lamella

P_{CB} : capillary pressure at Plateau border

P_A : liquid pressure at center lamella

P_B : liquid pressure at Plateau border

P_G : pressure in gas- phase

Since $R_{1A} > R_{1B}$ as explained above, according to Young-Laplace equation:

$$P_{CA} < P_{CB}$$

From equation (1) and (2) and assuming that gas pressure is the same within a given bubble, we have:

$$P_A > P_B \qquad (3)$$

Equation (3) implies that liquid pressure at center lamella is greater that at Plateau border. This pressure difference enables film thinning by driving liquid out of lamella and causes it to rupture, resulting in foam coalescence.

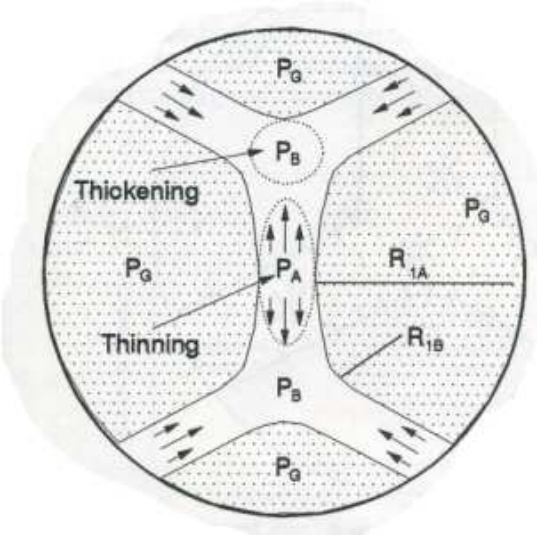

Figure 2.10 – Pressure differences across curved surfaces in a foam lamella (from Schramm, 1994)

2.1.6.2 Gas Diffusion

Trapped bubbles in porous media usually experience this mechanism. Young-Laplace equation suggests that gas on the concave side of a liquid film (lamella) is at

higher pressure than that on the convex side. Thus, there is a high chemical potential for gas to dissolve into the lamella and escape by diffusion from concave to convex side of a lamella. The rate of diffusion is proportional to film curvature squared and, of course, more rapid for small bubbles (Bikerman, 1973; Chambers and Radke, 1991).

In the case of confined foam in porous media, inter-bubble diffusion is much more complicated. This is because moving lamellae are continuously reshaped by the pore network since their curvatures are determined by pore geometries and flow properties for a given bubble size distribution (Nguyen *et al.*, 2004). However, gas diffusion might be negligible in high foam flow rate where convection is the dominate flow regime.

2.1.6.3 Oil Effect

The presence of oil has opposite effects on foam, stabilizing or destabilizing. However, detrimental effect of oil on foam stability is more like dominant. Therefore, the understanding of foam-oil interactions is very important when foam is used for mobility control in EOR.

This topic has gained intensive attention from researchers in the past few decades, as the increasing number of publications in this area shows. Some possibilities for mechanisms of foam destabilization by oil can be (Schramm, 1994):

- Liquid depletion in lamellae caused by absorption or adsorption of surfactant into oil phase, especially if there is emulsification.
- Rock wettability is changed by oil, thus make it harder for foam generation or re-generation.
- Spontaneous spreading of oil on lamellae that causes displacing of foam stabilizing interface.
- Emulsified oil drops breach and rupture the foam stabilizing interface.

The first two mechanisms are more likely related to phase behavior of surfactant-crude oil system, and have been shown to be insignificant for a number of

hydrophilic surfactants. Therefore, only the last two theories are responsible for destabilization of foam.

2.1.6.4 Other Factors Affecting Foam Stability

Surfactant Concentration

The use of surfactant stabilizes lamellae, thus increasing foam stability. This ability of surfactant can be explained by reviewing its structure.

In the most common form, surfactant consists of two parts: a hydrocarbon "tail" (non-polar) and an ionic "head" (polar). The hydrocarbon can be either a straight or branched chain. The tail of surfactant is hydrophobic and thus prefers to stay in non-polar media such as oil and gas. In contrast, the head of surfactant is hydrophilic and interacts strongly with polar environment such as water. Consequently, when added into two-phase system such as air/water or oil/water, surfactant tends to adsorb at the interface, resulting in reduction of interfacial tension (IFT) between two phases. However, there is a specific concentration called critical micelle concentration (CMC) below which the dissolved surfactant molecules are dispersed as monomers at the interface, and ITF is dramatically reduced. Above CMC, additional surfactant molecules result in formation micelles and cause very little change in IFT (figure 2.11a and 2.11b).

If the surfactant in use is ionic, the absorbed molecules will produce a surface charge on the interface, which consequently results in electrostatic repulsion force between opposite interfaces across a lamella (figure 2.12). This force is the primary stabilizing factor for lamella in the presence of surfactant. The combination of repulsive and attractive forces within a lamella is called *disjoining pressure*, $\Pi(h)$. This pressure is a function of lamella thickness and tends to counterbalance the suction capillary pressure at the film Plateau border (which causes thinning process). If it could, a stable lamella would be obtainable.

The increase in capillary pressure causes the film thickness to decrease, corresponding to the increase of disjoining pressure. The film will reach to critical

thickness when capillary pressure equals to maximum disjoining pressure, Π_{max}. If capillary pressure exceeds Π_{max}, the film ruptures.

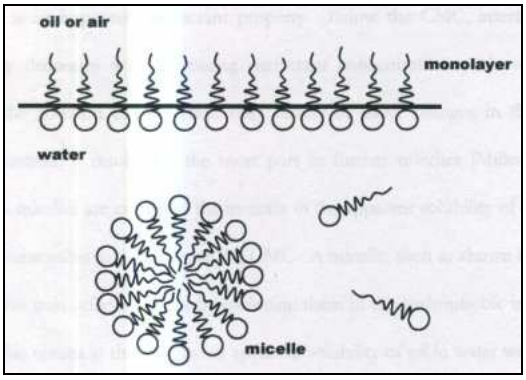

a)

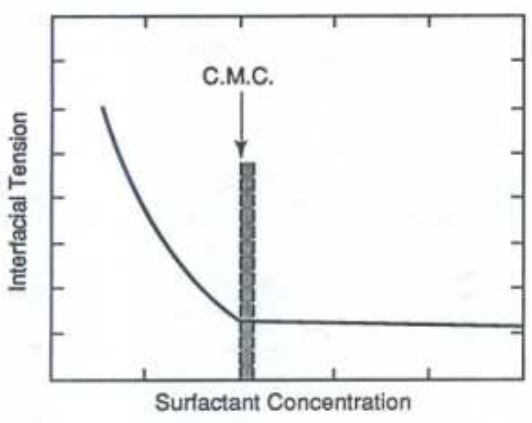

b)

Figure 2.11 – a) Surfactant behavior above CMC (Tanzil, 2001), and b) IFT as a function of surfactant concentration.

In the absence of oil, surface rheological properties at gas-liquid interface play an important role in foam stability when surfactant is added at concentrations below CMC. Upon the approach of two bubbles, lamella thinning process starts as liquid is driven out of lamella into Plateau borders by capillary pressure acting normal to the surfaces (as explained in section 2.1.6.1). This flow of liquid creates a convective-flux

of surfactant in the sub-layer (Schramm, 1994). Consequently, surfactant concentration at the surface is increased in the direction of the flow, and thus surface tension is reduced. This surface tension gradient produces a force opposite to the flow of liquid, causing lamella to regain its original configuration. This restoration is known as Gibbs-Marangoni effect.

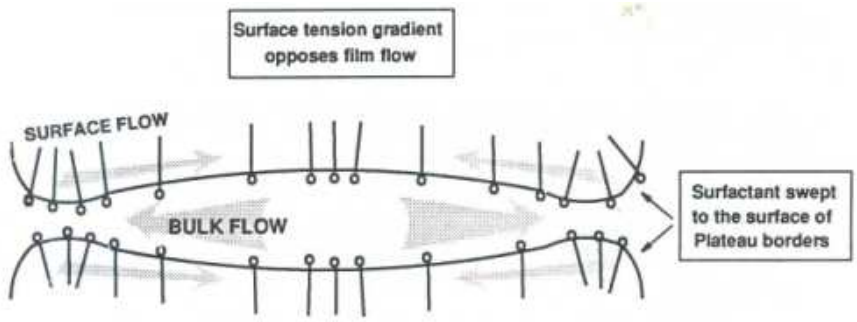

Figure 2.12 – Demonstration of Gibbs-Marangoni effect on film drainage process

In contrast, at concentrations several times higher than CMC, the role of surface rheological properties becomes insignificant. However, many studies, for example Bikerman *et al.,* (1978), have shown that foam stability increases with increasing surfactant concentration even far beyond CMC. Wasan *et al.,* (1994) explained this phenomenon by introducing another foam-stabilizing mechanism: ordered microstructure formation (stratification) in lamellae. This mechanism has brought a new understanding of foam stability to the oil industry where surfactant concentration is much higher than CMC in most of chemical EOR applications.

Temperature

The effect of temperature on foam stability is very important. The rate of stratification increases at high temperature, thus the drainage time is decreased. This means a lamella needs shorter time to coalesce. In contrast, a decrease of temperature can make stratification stop at larger thickness to increase lamella stability (Wasan, 1994).

2.2 ALKALI – SURFACTANT – GAS (ASG) PROCESS

Alkali – Surfactant – Gas process shares the same concept with chemical EOR flooding, which is reducing capillary forces that are responsible for phase trapping in porous media through the use of surface active agents, or surfactants. The implementation of alkali and gas in ASG only makes the process more robust and effective in microscopic displacement, which results in higher reduction of residual oil saturation S_{or}. This section presents the basic concepts applied in ASG, which are also well-known in chemical EOR, as well as the main chemicals used in the process. Upon the completion of part, the readers will have a clear vision about ASG process and be able to fully understand the materials contained in Chapter 4.

2.2.1 Basic Concepts

2.2.1.1 Capillary Forces and Capillary Number

Capillary Forces

It is well-known that high capillary forces are responsible for trapping of oil in porous space, resulting in poor microscopic displacement efficiency in water-flooding. These forces originate from the contrast of water and oil viscosities, and consequently large interfacial tensions (ITF) existing between these two phases.

Capillary pressure is defined as the pressure difference exists across the interface of two phases and described as:

$$P_c = \frac{2\sigma_{ow}\cos\theta}{r} \tag{2.4}$$

where: P_c = capillary pressure

σ_{ow} = IFT between oil and water

θ = contact angle

r = capillary tube radius

Clearly from equation (2.4) that capillary pressure is related to fluid/fluid interfacial tension (IFT), wettability of rock (through θ) and size of capillary, r. In porous media, r represents pore throat radius and can not be changed. Thus, reducing capillary pressure through lowering fluid/fluid IFT is likely the only feasible method.

The idea of using chemicals to reduce capillary pressure by lowering interfacial tension (IFT) of a brine/oil/rock system started the concept of chemical EOR process. This type of EOR uses surface active agents (as surfactants, for short) for the purpose of effectively achieving such low IFT for a given brine/oil/rock system. As technology and understanding of chemicals proceeded to advance, chemical EOR has evolved into various types. The differences come from chemical compositions, volume of primary injected slug, addition of alkali or co-solvent, etc. However, the main purpose is still the same, that is, to lower IFT for significant reduction in S_{or}.

Capillary Number

Displacement of residual phases, in this case residual oil, is strongly effected by IFT and correlated as a function of capillary number N_c, a ratio between viscous and capillary forces, expressed as:

$$N_c = \frac{v\mu_w}{\sigma_{ow}} = \frac{F_v}{F_c} \qquad (2.5)$$

where: F_v and F_c = viscous and capillary forces, respectively

v= interstitial velocity

μ_w = viscosity of water

σ_{ow} = IFT between oil and water

As suggested from equation (2.5), a decrease in IFT leads to increasing of capillary number. This reverse relationship is shown in figure 2.16, where residual oil saturation S_{or} is effectively reduced with increasing capillary number N_c (data were gathered from several authors). However, it also appears from figure 2.16 that S_{or} only reduces after N_c has reached relative high values (around 10^{-4} or 10^{-3} and even higher if displaced fluid is non-wetting). Many studies have proven that such values can be practically achieved when IFT is lowered to around 10^{-2} dynes/cm.

Alkali – Surfactant – Gas process shares the same concept with chemical EOR flooding as discussed above. The implementation of alkali and gas in ASG only

makes the process more robust and effective in microscopic displacement, which results in higher reduction of residual oil saturation S_{or}.

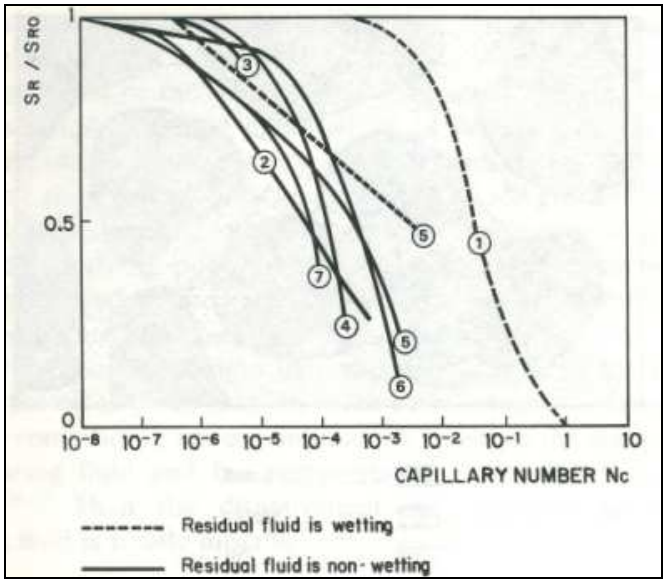

Figure 2.13 – Relationship between residual oil saturation and capillary number (data gathered from several authors – Curve 1: Dombrowski & Brownell; Curve 2: Moore & Slobod; Curve 3: Wagner & Leach; Curve 4: Taber; Curve 5: Lefebvre du Prey; Curve 6: Foster; Curve 7: Abrams)

2.2.1.2 Microemulsion Phase Behavior and Interfacial Iension (IFT)

Microemulsion Phase Behavior

Microemulsion phase behavior is the concept used to characterize the behavior of a particular surfactant/oil/brine mixture, or microemulsion system. Through the use of surfactants, such a system can have ultra low IFT with either aqueous or hydrocarbon phase. Healy and Reed (1976) found that low IFT values correlate with high solubilization of oil and water, which is of interest since more residual oil is potentially solubilized. Therefore, studying microemulsion phase behavior is very important in order to locate regions of high solubilization.

Microemulsion phase behavior is very complicated and dependent on many parameters. Most important parameters are: types and concentrations of surfactants,

hydrocarbons; brine compositions, especially brine salinity; and temperature. Unfortunately, there is no equation of state to model such a simple microemulsion system. Thus, microemulsion phase behavior must be studied experimentally, and results are typically presented in graphs.

Healy *et al.,* (1976); Nelson and Pope, 1977; and Nelson *et al.,* (1979) found that salinity had a significant effect on microemulsion phase behavior. Generally, increasing salinity decreases solubility of ionic surfactants. Thus, they characterized microemulsion phase behavior into three types: Type I, Type III, and Type II, corresponding to increasing salinity (figure 2.17).

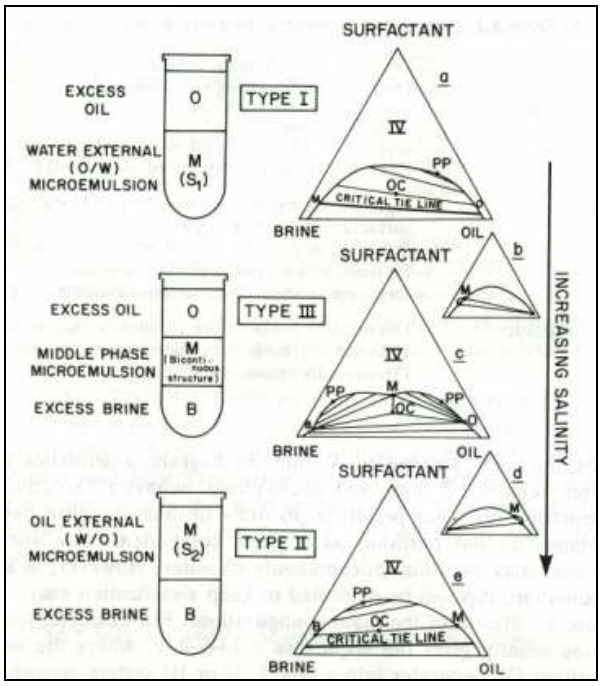

Figure 2.14 – Microemulsion phase behavior and the effect of salinity (Pope and Baviere, 1981)

In Type I, where salinity is low and most of surfactant molecules stay in aqueous phase, the system appears with excess oil phase on top of water-external microemulsion which contains a very small amount of solubilized oil (figure 2.17 a). This type of microemulsion is usually called lower phase microemulsion.

At high salinity, or Type II microemulsion, the electrostatic forces dramatically push surfactant from aqueous phase into oleic phase to form water-in-oil

microemulsion. The system at this salinity contains an excess aqueous phase at the bottom and water-in-oil microemulsion on the top (figure 2.17 e), and is referred as upper phase microemulsion.

In Type III (intermediate salinity), the system behavior becomes very complex with the existence of water, oil, and microemulsion phases (figure 2.17 c). The microemulsion phase stays between and is in equilibrium with both oil and water. This type is called middle phase microemulsion. The lowest IFT values are found within the salinity range of Type III.

Interfacial Tension (IFT)

There is a strong relationship between microemulsion phase behavior and IFT of equilibrium phases, as well as between IFT and solubilization of water and oil by microemulsion, according to Healy and Reed (1977). Therefore, it is reasonable to say that IFT is also a function of salinity and can be demonstrated through solubilization parameters. Figure 2.18 is the plot of IFT and solubilization parameters versus salinity. The symbol σ_{mo} represents IFT between microemulsion and excess oil, whereas σ_{mw} stands for IFT between microemulsion and excess water. Solubilization parameters V_o/V_s and V_w/V_s define the volume of oil and water solubilized by microemulsion, respectively, and are described as:

$$SP_o = V_o / V_s = \frac{\text{volume of oil in microemulsion phase}}{\text{volume of surfactant in microemulsion phase}}$$

$$SP_w = V_w / V_s = \frac{\text{volume of water in microemulsion phase}}{\text{volume of surfactant in microemulsion phase}} \qquad (2.6)$$

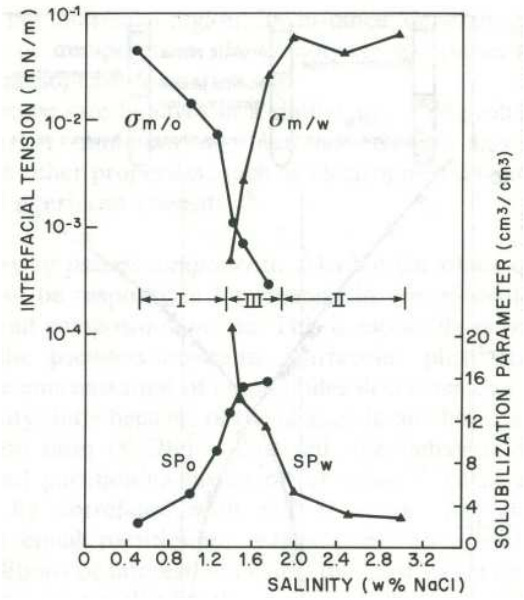

Figure 2.15 – Solubilization versus salinity

As seen from the plot, σ_{mo} and σ_{mw} exhibit different trends with salinity change. As salinity increases, σ_{mo} decreases as the phase behavior proceeds from Type I (lower phase) to Type III (middle phase) and toward Type II (upper phase). This change corresponds to increasing solubilization of oil from excess oil to microemulsion, resulting in lower-density microemulsion. The reverse trend is observed for σ_{mw}. An increase appears in σ_{mw}, corresponding to decreasing solubilization of water as the system goes from middle phase to upper phase. The salinity at which two curves cross, or $\sigma_{mw} = \sigma_{mo}$, is called optimum salinity where lowest IFT values between phases are usually found (Healy and Reed, 1977).

Also seen from the figure is that optimum salinity for IFT is relatively equal to that for phase behavior, which is defined at $V_o/V_s = V_w/V_s$. This observation simplifies the direct measurement of IFT which is difficult and in the need of special instruments. Instead, solubilization parameters can be calculated from equation (2.6) based on known information received from screening phase behavior through a series of pipettes (will be introduced in chapter 3). Then IFT will be computed through solubilization parameters by using reliable models such as Chun-Huh's model or Healy and Reed's model (1974).

2.2.1.3 Mechanism and Mobilization of Residual Oil

During tertiary flooding, a specified volume of chemical slug containing surfactants with designed concentrations and is injected at optimum salinity (usually at Type III microemulsion), followed by a drive solution with lesser surfactant concentration and lower salinity (within Type I). Mobility control is provided by co-injecting or alternate injecting of gas with both slug and drive solutions to generate foam. Formation of foam is responsible for gas trapping in porous media and lowering liquid relative permeability (through decreasing liquid saturation as discussed in section 2.1.5). Chemical slug is, therefore, diverted into lower permeable regions where residual oil resides after waterflood. Reaction between surfactants in the slug and oil leads to formation of microemulsion at the displacement front, which has ultra low IFT with both oil and water. As the chemical slug proceeds through porous media, more oil and water is solubilized into the microemulsion, resulting in the mobilization of residual oil, as well as the formation of an oil bank right in front of microemulsion phase. As long as the microemulsion slug is still able to solubilized oil and water, the flow remains as a single phase.

Microemulsion and oil bank is pushed through porous paths by co-injection or alternate injection of drive solution and gas. Foam generated in this step is for improving displacement and sweep efficiencies.

2.2.1.4 The Concept of Salinity Gradient

One of the first studies on salinity gradient was done by Nelson *et al* (1983). Since then, the concept has become very popular and widely used due to its effectiveness in improving oil recovery in chemical EOR. Moreover, the concept was used in this thesis, therefore, it is necessarily to introduce it to the readers.

In his work, Nelson conducted four tertiary floods with different salinity gradients. The results from both experiments and simulations suggested that system with negative salinity gradient gives better recovery and acceptable surfactant retention. Details are presented below.

- *Under-optimum salinity system*: salinity is designed to keep surfactant in under-optimum or Type I environment. It is obvious that within this type surfactant stays in aqueous phase. Thus, less surfactant will be in contact with oil and IFT is not low enough for good oil displacement to happen.

- *Over-optimum salinity system*: salinities in slug and drive solutions are such that the flood will exist throughout an over-optimum or Type II environment. This design shows some disadvantages. First, IFT is still high for mobilization of residual oil. Second, Type II environment retards the transport of surfactant since surfactant is being absorbed into trapped oleic phase. Therefore, surfactant is not carried to the location where it is required to displace oil bank, resulting in poor displacement efficiency.

- *Constant salinity system*: has the same salinity in formation brine, slug and drive. As observed from experimental and simulation results, most of surfactant is trapped by being absorbed into trapped oleic phase, which is the same situation happens in over-optimum system. Moreover, early breakthrough of surfactant also occurs.

- *System with negative salinity gradient*: slug is injected at optimal salinity while the drive salinity is, at most, equal to optimal salinity when there is no surfactant (figure 2.17; Nelson, 1983). The idea is to form Type II in front of surfactant bank. Surfactant will be absorbed into trapped oleic phase in Type II environment and therefore its transport is retarded. Then, the drive with salinity in Type I will transport both the surfactant and emulsified oil back into aqueous phase.

From observing experimental simulation results, Nelson also concluded that negative salinity gradient system has several advantages over the other systems, such as: (1) salinity profile goes through optimal salinity; (2) reduce surfactant retardation by trapping it in Type II environment in front of surfactant bank; (3) low salinity in drive solution transports both surfactant and emulsified oil back into aqueous phase and flows as single-phase.

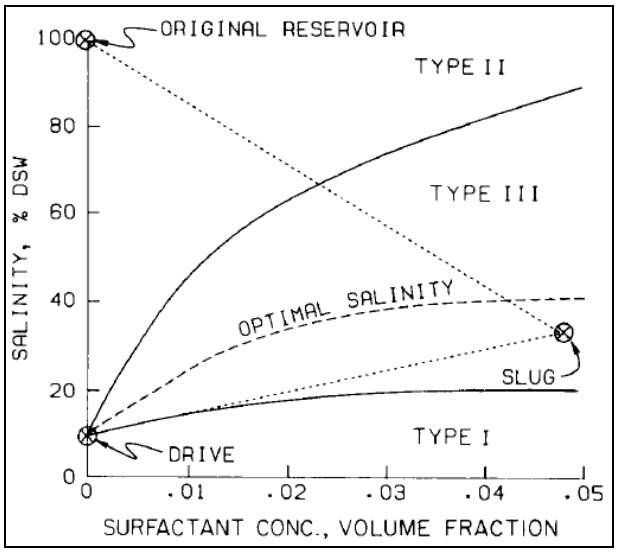

Figure 2.16 – Schematic of salinity gradient concept (obtained from Nelson, 1983; modified by Nhut Minh Nguyen, 2010)

2.2.2 Chemicals used in the Process

2.2.2.1 Surfactants

Surfactants are defined as chemical substances that concentrate at the interface of two immiscible fluids when added at low concentration. This ability allows surfactants to alter interfacial properties significantly, such as reduce surface tension, or IFT.

In the most common form, surfactant consists of two parts: a hydrocarbon "tail" (non-polar) and an ionic "head" (polar). The hydrocarbon can be either a straight or branched chain. The tail of surfactant is hydrophobic and thus prefers to stay in non-polar media such as oil and gas. In contrast, the head of surfactant is hydrophilic and interacts strongly with polar environment such as water.

Surfactants can be divided into four groups based on the ionic nature of the head, as below:

- *Anionic*: the head is negatively charged, such as sodium dodecyl sulfate ($C_{12}H_{25}SO_4^-Na^+$). This type of surfactant has been widely used in EOR application since it has low adsorption on rock surface, good properties,

and is relatively stable. More importantly, it can be produced economically.

- *Cationic*: this surfactant has positive charge on its head. For example, dodecyltrimethylammonium bromide ($C_{12}H_{25}N^{+}Me_3Br^{-}$). Cationic surfactants are rarely used due to strong adsorption on rock surface.
- *Nonionic*: this molecule does not ionize. The head group is larger than the tail group. One of examples can be dodecylhexaoxyethylene glycol monoether ($C_{12}H_{25}[OCH_2CH_2]_6OH$). Surfactants of this type are usually used as co-surfactants to improve phase behavior of microemulsion systems. They have much higher salinity tolerance but lower ability of IFT reduction, compared to anionic surfactants.
- *Zwitterionic*: two groups of this surfactant have opposite charge. Such as 3-dimethyldodecylamine propane sulfonate.

When added into two-phase system such as air/water or oil/water, surfactant tends to adsorb at the interface due to its unique structure and properties as discussed above. This results in the formation of microemulsion in which both water and oil are solubilized. In optimum conditions of surfactant compositions, temperature and salinity, microemulsion can possess ultra low IFT with both water and oil, which accounts for the mobilization of water and residual oil in EOR application.

In order to improve performance of surfactants, neutral groups or intermediate groups are sometimes added to carbon chain of surfactant. For example, addition of hydrophobic groups such as propylene oxide (PO) lowers optimum salinity and increases calcium tolerance of a surfactant with respect to a given oil, temperature, and salinity. Similar effects can be achieved by tailoring ethylene oxide (EO) or both EO and PO groups to a surfactant.

2.2.2.2 Alkali

The use of alkalis was first proposed from early 1920s. Even though the acting mechanisms were not well-understood at that time, the hypothesis of changing

wettability combined with reducing oil-water IFT was emitted (Labrid, 1991). Later on, mixing of alkalis and surfactant has gained considerable interest and become a popular process for EOR application (Nelson *et al.,*1984; Peru and Lorenz, 1990; Surkalo, 1990; Baviere *et al.,* 1995).

The main role of alkali is to reduce the adsorption of anionic surfactants (Wesson and Harwell, 2000), and sequester divalent cations. Another benefit of using alkali is that soap can be generated in-situ due to the reaction of alkali and naphthenic acid in reactive crude oil. Thus, surfactant can be injected at lower concentration than if used alone since soap acts just like another source of surfactant, making the process more economical. Moreover, the use of alkali has been proven to be capable of changing rock wettability. This benefit is very important in making an effective EOR process for fractured oil-wet reservoirs.

However, alkali was not used throughout this particular study. Therefore, the author only presented a brief introduction of alkali but not all topics related to this chemical.

2.2.2.3 Co-Solvent

Co-solvents, usually alcohols, are small carbon chain alcohol molecules that act at the oil-water interface of microemulsion droplets to reduce the viscosity of microemulsion and prevent the formation of gel-like phases separating from surfactant solution. Addition of hydrophilic alcohols also helps to increase the solubility of surfactant in high salinity environment. However, disadvantages of using alcohols were soon reported. It reduces solubilization of oil and water in microemulsion, thus increases the IFT originally achievable with a given surfactant. (Salter, 1977) and shifts the optimum salinity to a higher value.

More importantly, alcohols destabilize foam that is used for mobility control in the injection of slug and drive solutions. However, for temperature below 60^0C, the use of alcohols can be reduced or eliminated by: (1) branching the hydrocarbon chain of surfactant, (2) adding ethylene oxide (EO) or more hydrophobic propylene oxide

(PO) groups, (3) blending surfactants with different structures and carbon chain lengths.

2.2.3 Literature Review of ASG Process

The concept of foam as a means for mobility control was introduced 30 years ago by Lawson and Reisberg (1980). In their study, foam was generated by alternatively injecting of an inert gas and surfactant solution. During slug injection, gas slug to surfactant slug ratio was kept at 1:1, and surfactant slug varied from 0.1 PV to 0.25 PV. In the drive injection, both gas and surfactant slugs were maintained at 0.1 PV. Experimental results were favorably compared to the case in which water-soluble polymers were used to highlight the potential of using foam for mobility control.

Later, Rossen and Zhou (1992) studied and modeled the foam diversion in matrix acidization process on sandstone rocks. Their findings were that the greatest diversion could be obtained when foam is preceded by surfactant pre-flush then followed by an acid slug that is compatible with foam. They also concluded that the key to success of such a process is the ability of surfactant solution to immobilize the gas in previously injected foam.

Recently, Quoc and Viet (2008) performed a series of experiments on carbonate rocks to study the injection strategy for foam generation. In their work, several injection strategies were implemented, including conventional SAG (surfactant alternating gas), novel WAGs (water alternating gas with surfactant injected in CO_2), and novel CO_2 (continuous CO_2 injection with dissolved surfactant). The results indicated that foam was generated in all injection strategies. Moreover, CO_2-dissolved surfactant injection greatly reduced gas mobility compared to conventional injection strategies, which pointed out the potential of foam as mobility control agent.

About the same time, Feng Li (2008) also demonstrated the use of foam for mobility control through a series experiments on layered sandpack with different permeability ratio between layers. Successful experiments data showed that a foamed-

drive can be an alternative for polymer drive in the mean of mobility control. Additionally, in the presence of foam, the vertical sweep of a layered sandpack was significantly improved with SAG injection compared to waterflood (without foam) or WAG.

One of successful foam field tests was Chevron's Rangely Weber Sand Unit, in northwestern Colorado (1988 – 1990). The foam project started in 1989 with the co-injection of CO_2 and surfactant slug. Foam was placed in reservoirs in spite of a large hydraulic fracture in injection well. Results showed that foam reduced CO_2 injectivity for 2 months during the CO_2 chase period.

Another successful field trial also came from Chevron's North Ward-Estes, in west Texas (1990 – 1991). Within this period, four cycles of SAG was injected into an injection well to generate foam. During these cycles, CO_2 injectivity was reduced by 40% to 85% together with a sharp decrease in CO_2 production. Apparently, in the presence of foam, CO_2 was diverted into the thief zones.

Mobil's Slaughter and Greater Aneth field trials (1991 – 1994) were additional successful indications of foam utilization. In this project, four CO_2-foam field trials were performed: two trials at Slaughter field (west Texas), the other two at Greater Aneth field in carbonate reservoir (south Utah). Two injection methods, SAG and co-injection, were tested. The outcomes in all cases highlighted sharp decrease in CO_2 injectivity and significant increase in oil production. Another conclusion was that co-injection method is more difficult to perform but more effective in reducing CO_2 mobility compared to SAG.

Summary of Literature Review on ASG

Careful screening of literature review on ASG process has led to the following conclusions:

- Most of previous studies on ASG process only stopped at observing foam as a mobility agent and lacked of indentifying optimal conditions where ASG can be performed effectively and economically.

- The effects of parameters involving in SG process such as permeability, pressure, injection quality and strategy, surfactant compositions, etc. have not been studied systematically.
- Oil was generally recognized as a defoamer. However, since negative salinity gradient concept is widely applied in chemical EOR together with the use of foam throughout the process, it is essential that foam stability at different salinity, corresponding to different microemulsion environments, needs to be fully understood.
- Least but no last, there has been only a few studies of ASG performed on carbonate reservoirs despite the fact that this lithology contains a significant amount of world's oil reserves.

Inspired by recognizing the gaps in ASG understanding as listed above, the author performed this study in order to partially fulfill those gaps, while hoping that in the near future a systematic study would be conducted to fully understand and discover the real potential of this process.

CHAPTER 3

DEVELOPMENT OF NEW TWIN TAILED SURFACTANT FOR SUPERCRITICAL CO_2 – WATER INTERFACE

3.1 BACKGROUND

3.1.1 Foam Flow in Porous Media

It has been established that when CO_2 and a suitable surfactant are injected into water-bearing porous media, foam is generated as a series of lamellae through a number of different mechanisms (Rossen 1996; Kim 2005; Apaydin and Kovscek 2001). These lamellae are responsible for reducing mobility of CO_2 by blocking flow paths and temporarily lowering gas permeability. The lamellae that are formed will generally move a certain distance before collapsing, and their behavior is primarily dictated by the designed surfactants.

The processes by which the lamellae are formed are dependent on shear rate and therefore the formation of the foam is a function of the velocity of the fluids in the pores. In essence, foam in porous media behaves as a shear thickening fluid. The consequence of this is that in areas of highest fluid flow the formation of foam will be greatest. Therefore in a reservoir with a high permeability contrast, the effect of foam should generally be to balance out the flow of the fluids. Further, since drainage of lamellae caused by capillary forces and oil spreading on the lamellae surface are two of the major pathways to lamellae rupture, foams will tend to breakdown fastest where the permeability is lowest and oil is present.

3.1.2 Foam Stability vs. Formation Rate

The formation of foam is a shear dependent phenomenon and the propagation of the foam front is dependent both on the generation and rupture of lamellae. It is apparent that both processes need to be properly balanced when choosing a CO_2 foaming surfactant. The surfactant should stabilize the foam, but the length of time that the foam is stable is not of paramount importance. More importantly, the

preferred surfactant should be capable of creating foam at low shear rates. The foam front is a dynamic system, and its constituent lamellae are constantly being formed and destroyed as it propagates through the formation.

3.1.3 CO_2 Foaming Surfactants

Given the importance of the formation of the lamellae, it is surprising that nearly all of the screening tests for determining the best CO_2 – foam surfactant are solely based on the stability of the foam. Moreover, the screening tests have often done using air and water at atmospheric pressure. Not surprisingly therefore, the chosen surfactants were typically anionic alcohol sulfates and olefin sulfonates, which are very good at forming stable water/air foams, but have poor tolerance of salinity (most specifically dications such as Ca^{2+} and Mg^{2+}) and also suffer from adsorption on carbonate rocks (Lawson 1978 and Grigg and Schechter 1997). Non-ionic surfactants were generally considered to be inferior in terms of foam stability.

3.1.4 CO_2 Philic Surfactant Design

Over the last 50 years, a large number of commercially available surfactants have been tested for their ability to create CO_2/water emulsions. Until recently, however, most of the surfactants that have been tested in the application were commercial surfactants generally designed for lowering the interfacial tension between water and oil. Not until the 1990's was a significant effort put forth to develop surfactant specifically for the CO_2/water interface, and then most of those efforts were directed towards forming water in supercritical CO_2 microemulsions (Eastoe 2006 and Sagisaka *et a*l. 2004). Many of the surfactants designed for CO_2/water systems required fluorinated groups and were therefore came with EH&S as well as economic concerns (Consani and Smith 1990).

Recent work by the groups of Johnston and Enick have shown that non-fluorinated systems can be designed that are CO_2-philic (Adkins et al. 2010 and Wang et al. 2009). The key to designing a CO_2-philic molecule is to minimize intermolecular attractions while maximizing the interaction with the CO_2. Some of the

CO_2-philic features are: (1) low molecular weight hydrophobes, (2) branching, and (4) non-ionic.

3.1.5 Twin-tailed Surfactants

How surfactant molecules are oriented at the interface has large impact on interfacial tension. For linear surfactants at the air-water interface, strong tail-to-tail interactions tend to dominate and, due to the high surface tension at the water-air interface (typically 72 dynes/cm), provide a strong driving force for migration to the interface. This leads to low critical micelle concentrations (CMCs) and high efficiencies. Adding branched or double-tails lowers the packing ability, which reduces the tail-to-tail interactions and the driving force for the surfactant to adsorb at the interface. The net effect is for higher CMCs and lower efficiency for twin-tailed surfactants at the air-water interface.

Recently, Adkins *et al* (2010) has shown that the situation was not the same at the CO_2-water interface where lower interfacial tension (~22 dynes/cm) reduced the driving force for adsorption at the interface. In this situation, interaction of the tails with CO_2 was more important and leading to a greater driving force for adsorption of twin-tailed surfactants at the interface. More importantly, although it was found that the area occupied by the twin-tailed surfactants was very high, they were still very effective in lowering the interfacial tension (4 mN/m).

3.2 EXPERIMENT DESCRIPTION

3.2.1 Materials

3.2.1.1 Synthesis/Manufacture of Surfactants

The following reagents were purchased and used without purification: NaOH pellets (97%) (Aldrich); epichlorohydrin (Aldrich); and Chloroform-d (Cambridge Scientific). Additionally, n-Butanol (Fisher) was distilled and dried over 4Å molecular sieves prior to use. NMR samples were prepared by dissolving ~0.1g of material in 0.5mL of Chloroform-*d*. NMR Spectra were acquired using a Bruker

AVANCE spectrometer at 250 MHz for ^{1}H and 62.8MHz for ^{13}C. Spectra were referenced to the center peak of the $CDCl_3$ signal at 77 ppm for the ^{13}C and to the residual CHCl3 signal at 7.26 ppm for the ^{1}H spectra respectively.

1,3-Dioctylpropan-2-ol: the dioctylglycerine synthesis has been previously described in the literature (Thoen 2008).

1,3-Dibutoxypropan-2-ol: to a 1 liter three necked round bottom flask purged with nitrogen and fitted with a short path distillation adaptor was added 66.4g of sodium hydroxide pellets and ~700ml of anhydrous n-BuOH. The n-BuOH was distilled at 60^{o}-70^{o}C under 400 torr and vacuumed until ~100 ml of n-BuOH had been removed. The flask was back-filled with nitrogen and ~100 ml of anhydrous n-BuOH was added to give a clear yellow solution of n-BuONa. An additional funnel containing 63.8g of epichlorohydrin was placed on the flask and the flask cooled to 50ºC using a cold water bath. Epichlorohydrin was slowly added so that the temperature did not exceed 60ºC. Then, the solution was cooled down to room temperature and stirred for 12 hours. The solution was neutralized with 80g of HCl (conc) diluted with 100ml of distilled water. The product was filtered and the excess n-BuOH removed by distillation under vacuum. The product was filtered through a plug of aluminum oxide to yield 82g of a clear colorless oil. ^{1}H NMR (250 MHz, CDCl3): δ 3.89 (p, 1H), 3.41 (m, 8H), 2.88 (broad s, 1H), 1.51 (tt, 4H), 1.33 (dq, 4 H), 0.87 (t, 6 H);^{13}C NMR (62.8 MHz, CDCl3): δ 71.8, 71.1, 69.2, 31.5, 19.1, 13.7.

Dialkylglycerines were ethoxylated to desired degree in an autoclave reactor using either BF3 or Sodium Hydroxide as catalyst.

3.2.1.2 Equipments

The foam coreflood apparatuses are schematically shown in figure 3.1. It includes three main components: (1) CO_2 and aqueous solution injection system, (2) core holder and pressure transducers, and (3) backpressure and effluent collection system.

Fluid Injection System

Digital HPLC Dual Pump (model 1500) with maximum working pressure of 5000 psig was used to directly inject brine or surfactant solution. CO_2 was injected at a constant rate by another Digital HPLC Dual Pump (model 1500) through a floating-piston accumulator. Two accumulators of Model CFR-50-200 manufactured by the Temco were used, each of which has a floating piston driven by a displacing fluid (Dow Corning fluid). The pistons made from PEEK (Polyether-Ether-Ketone) is mechanically strong enough to work under high pressure and resistant to CO2 diffusion. Each piston had three grooves with o-rings to separate the Dow Corning fluid and CO_2. One accumulator was used for pure CO2 injection while the other contained CO2 with dissolved surfactant. The surfactant and CO_2 were mixed together in the latter accumulator by a mechanical mixer. Another HPLC dual pump was used to inject brine or surfactant solution.

Core Holder and Pressure Transducers

Phoenix Hassler-type core holder was mounted in the vertical direction and fluids were injected from the top to the bottom. Hydraulic oil was used as an overburden fluid, which compressed and sealed the ¼-inch-thick Viton rubber sleeve to assure the axial flow of the injected fluids. The core holder has two end caps one of which has an adjustable end plug length to accommodate different core lengths. There were three pressure taps along the core holder connected to two pressure transducers as shown in Figure . The pressure transducers measured the pressure drops over two sections of the same length (called Section 1 and 2) that constituted the core.

Backpressure Regulator (BPR) and Effluent Collector

A Mity Mite backpressure regulator (BPR) from Grove Valve and Regulation Company (Oakland, CA) was used to maintain a constant backpressure during coreflood experiments. Two BPRs were used for the experiment. One was installed at the CO_2 injection line operated at 1800 psi to provide a constant injection rate to the core. The other one was installed at the outlet of the apparatus operated at 1500 psi. The effluent was collected for determining oil recovery using a fractional collector.

3.2.2 Experimental Procedure

3.2.2.1 Core Preparation

Corefloods were performed on outcrop carbonate cores whose diameter and length were 2 in and 1 foot, respectively. The average permeability of cores was 80 md. Since high-pressure CO_2 could diffuse through the rubber sleeve into the overburden fluid, the core was wrapped in aluminum foil and a shrinking Teflon tube. A hand pump, Enerpac model P-391 (Rex Supply Corporation, Austin, TX), was used to exert confining pressure around the rubber sleeve. The wrapped core was then placed in the core holder whose outlet was connected to the vacuum pump, and inlet was closed. Both axial and radial confining pressures were maintained to force the Teflon tubing, aluminum foil, and the sleeve into good contact. The core was vacuumed for 10 hours to make sure there was no air trapped in the core before measuring core porosity and saturating the core with formation brine.

3.2.2.2 Porosity Measurement

The core outlet was disconnected from the vacuum pump and then connected to a burette that was filled with a brine solution through a 3-way valve. The brine level in the burette was recorded. The total volume of brine imbibed into the core could be calculated by the differences in brine levels. To determine the pore volume of the core, the dead volume due to tubing lines must be subtracted from the total volume.

3.2.2.3 Core Saturation Procedure

After performing porosity measurement, the inlet was connected to the HPLC pump and brine solution was injected at 2 ml/min into the core while the outlet remained closed. Once the core pressure increased to the atmospheric pressure, the outlet was opened to the BPR set at 1500 psi throughout all experiments. The brine injection stopped after 10 injected PV.

3.2.2.4 Permeability Measurement

The core permeability was measured with 1 wt% NaCl solution after the porosity measurement. Permeability measurement is based on Darcy's law, which can be rearranged into the following form:

$$\frac{q\mu}{A} = k\frac{\Delta P}{L} \tag{3.1}$$

where q is the flow rate; μ the viscosity of fluid; A the cross-sectional area of the core; k the permeability; ΔP the pressure drop along the core; and L the length of the core. Normally pressure drops at different flow rates are measured. Then $q\mu/A$ is plotted versus $\Delta P/L$. A straight line, forced to go through the origin, can be fitted into the data; the slope of the line represents the permeability of the core. If the data deviate significantly or systematically from the linear trend, there may have been an experimental artifact in the data.

3.2.2.5 Foam Injection

Foam was generated in-situ by co-injecting CO_2 and 0.2 wt% surfactant solution (i.e. active concentration) in the presence of 1%wt NaCl. The superficial velocity of the liquid was 1 ft/day and the foam quality at 1500 psi backpressure was 90%. All corefloods were conducted at 45^{o}C.

3.3 RESULTS & DISCUSSIONS

3.3.1 Surfactant Structures

The synthesis of the dialkyl glycerine surfactants were carried out using the process described by Thoen using octanol or butanol, respectively, and epichlorohydrin (Thoen 2008). The dialkyl glycerines were subsequently ethoxylated to various lengths of EO using standard catalysis. For comparison, some data on primary alcohol ethoxylates and the Tergitol 15-S series of linear secondary alcohol ethoxylates have been included for reference. All chosen surfactants have linear alkyl chains and the branching therefore comes only from the position of the hydroxyl

functionality along the chain or through the inclusion of the glycerol linkage. The structures of the dialkylglycerine based surfactants are shown in figure 3.2.

3.3.2 Interfacial Properties

The CMC and interfacial tension data for the surfactants is tabulated in table 3.1. Rosen previously showed that changing from the linear alcohol ethoxylates ($C_{12}E_{12}$ and $C_{12}E_7$) to the secondary alcohol ethoxylates (15-S-12 and 15-S-7) the CMCs decrease slightly due to the poorer packing of the pseudo branched chains (Rosen 1982). The branching interferes with the surfactants ability to associate with itself and therefore the surfactant will have a more difficult time forming a micelle. This effect is muted as the EO chain increases in length and the hydrophilic head group begins to have a greater influence on the packing of molecules.

Johnson recently showed that this effect does not always correlate to other interfaces such as the $scCO_2$-water interface. He also found that due to the reduced interfacial tension was already present at the interface of $scCO_2$-water, the driving force for surfactant towards the interface based solely on their tail-tail interactions was muted and that the interaction of the hydrophobe with the CO_2 phase becomes more important for not only effectiveness (lower λ_{cmc}) but also for efficiency (lower C_{20}) (Adkins 2010).

As expected at the air-water interface, changing from a dioctylglycerine to a dibutylglycerine leads to a surfactant with a poor efficiency, as can be observed for the relatively high CMCs. Comparison with the corresponding 15-S series where the carbon length is closer to that of dibutyl glycerine (C_{11} vs $C_{12\text{-}14}$) shows that the efficiencies are close to an order of magnitude lower. In contrast, the effectiveness, as observed through the λ_{cmc} is relatively unaffected.

3.3.3 Foam Formation

To form a new lamellae, a certain work needs to be done to increase the interfacial area. The amount of work required to change the interfacial area (dA) is described by the following equation:

$$dW = \lambda dA \qquad (3.2)$$

Therefore, minimizing the interfacial tension is required to create a new interface with the least amount of work. However, this is not the only factor, but if the goal is to create foam as far from the injection well as possible where there is little fluid flowing and the energy available to do work is greatly diminished, it needs to be considered a critical parameter. For this reason, the dioctylglycerine (DOG-9) surfactants, which Adkins *et al*., (2010) showed to have very low C/W interfacial tensions (4mN/m) was chosen for the coreflood experiments (Adkins 2010).

3.3.4 Cloud Point

Typically, non-ionic surfactants are used at temperatures below their cloud point in the aqueous phase. The thought being that if the surfactant is not solubilized in the water then it will adsorb out on the rock surface. It could be speculated that if a surfactant contained a hydrophobe of high CO_2-philicity, the effect of utilizing the surfactant above the cloud point would drive the surfactant to the C/W interface. Therefore, surfactants chosen for the core flood experiments were utilized at temperatures approximately 15°C above their cloud points.

3.3.5 Core Flooding

Figure 2.3 shows the pressure drop over the two sections of the core during co-injection of CO_2 and 15-S-7 surfactant solution at 90% foam quality. The pressure drop in Section 1 first increased gradually and then more sharply after 1 pore volume (PV). Foam started to propagate into Section 2 as indicated by an abrupt increase in pressure drop after about 2.5 PV, while it continued to develop in Section 1. Pressure drop in both sections converged and simultaneously leveled off after about four PV,

signifying the onset of steady state foam flow. Steady-state foam yielded a pressure gradient of about 3.5 psi/ft, which was about 7 times pressure gradient induced by brine-CO_2 flow in the absence of surfactant. In other words, the total mobility reduction factor is about 7 for the foam stabilized by the 5-S-7 surfactant.

However, DOG-9 surfactant yielded much stronger foam as indicated by the pressure drop profile (figure 3.4). As clearly seen from the figure that pressure drop rapidly increases in Section 1 and then levels off when it starts to increases in Section 2 at around 0.6 PV. Gas broke through when the pressure drop in section 2 leveled off at around 1 PV. This indicates a sharp foam front advanced along the core at a velocity equivalent to the total superficial velocity of the injected gas and liquid. Moreover, figure 3.4 also shows that the steady-state pressure gradient is about 8 psi/ft, which is almost twice that for the 15-S-7 surfactant stabilized foam. Therefore, the effectiveness of DOG-9 surfactant in foaming CO_2 is significantly higher than that of the 15-S-7 surfactant.

Although both surfactants were injected at temperatures above their cloud points, neither causes plugging in the core, as is evident from the steady state pressure drops. Both cores attained steady state and foam was observed at the outlet in both cases. This evidence suggests that indeed driving the surfactant from the water does not necessarily cause precipitation to occur.

3.3.6 Conclusions

In this study, the twin-tailed dioctylglycerine surfactants were compared to a linear secondary alcohol surfactant through coreflood experiments. The results show that even above the cloud point of the surfactants, the twin tailed surfactant (DOG-9) creates a significant mobility reduction, likely due to favorable partitioning into the CO_2 phase. The data covers surfactant structures designed specifically for the CO_2-water interface. It can be used by producers and service companies in designing new CO_2-floods, especially in areas that might not have been considered due to problems with reservoir heterogeneity.

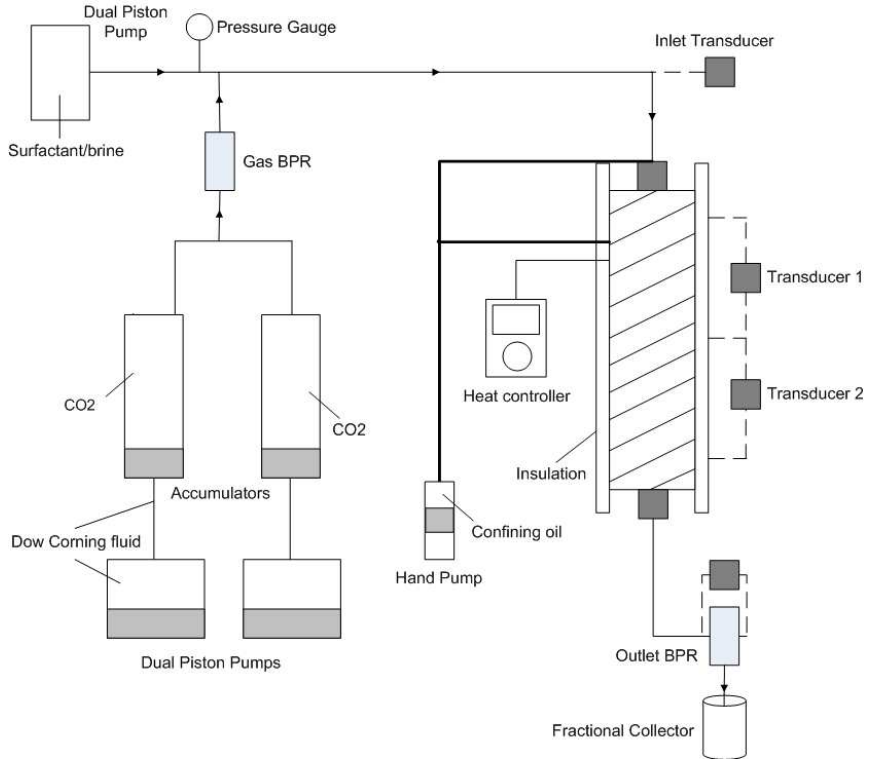

Figure 3.1 – Schematic of experiment setup for foam flooding

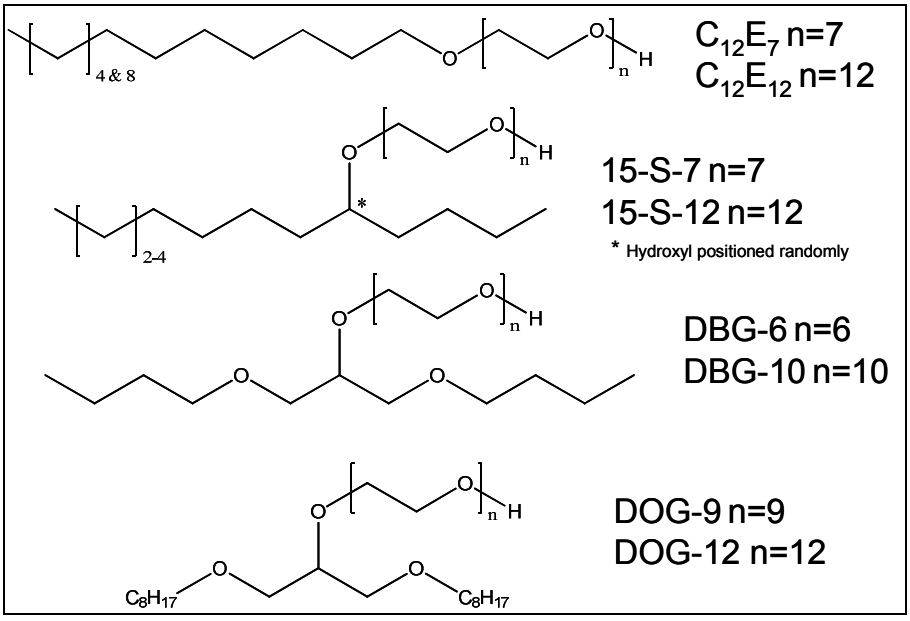

Figure 3.2 – Structures of surfactants

Table 3.1 - CMC and Surface Tension Data for Selected Surfactants

Surfactant	CMC	Surface Tension (mN/m)	Reference
$C_{12}E_7$	6.40E-05	30.9	Rosen 1982
$C_{12}E_{12}$	1.25E-04	38.3	Rosen 1982
15-S-7	2.92E-04	30.0	Dow
15-S-12	1.43E-04	33.0	Dow
DOG-9	8.43E-06	27.2	-
DOG-12	1.90E-05	27.5	Adkins 2010
DBG-6	1.00E-02	32.0	-
DBG-10	7.00E-03	35.0	-

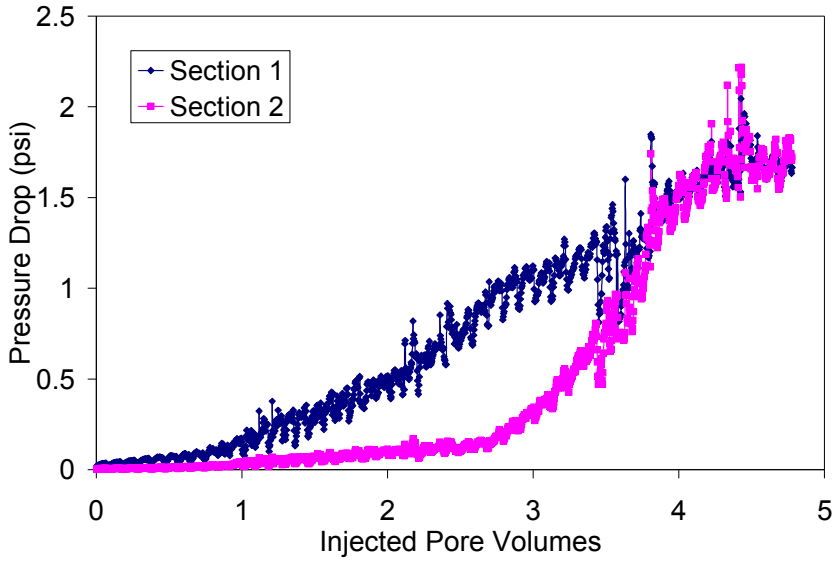

Figure 2.3 – Pressure drop profiles over Section 1 and Section 2 of the core during co-injection of CO_2 and 15-S-7 surfactant solution

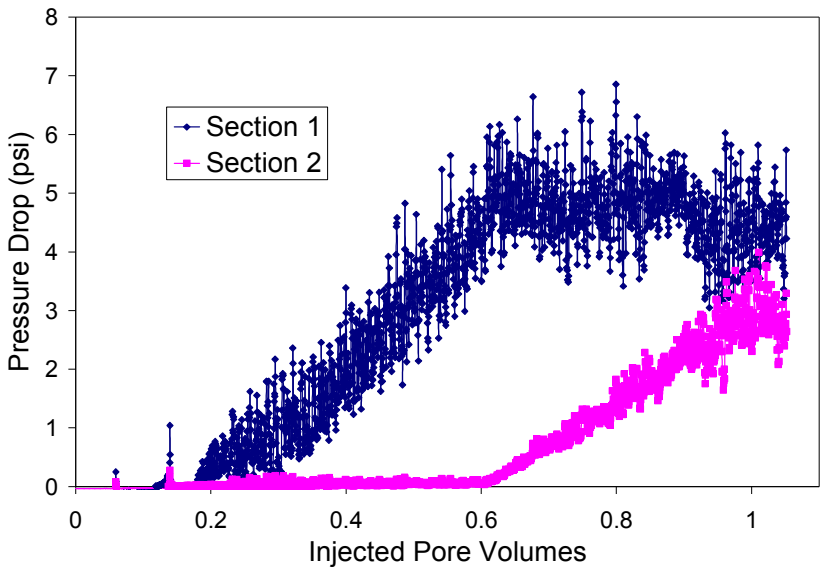

Figure 3.4 – Pressure drop profiles over Section 1 and Section 2 of the core during co-injection of CO_2 and DOG-9 surfactant solution

CHAPTER 4

EXPERIMENTAL STUDY OF ASG PROCESS ON CARBONATE ROCKS

4.1 INTRODUCTION

Previous chapters have introduced fundamental background and the potential of Alkali – Surfactant – Gas (ASG) process as a novel technique for chemical EOR. Also, as pointed out in Chapter 2 that there are only quite a few studies of this process have been done on carbonate rocks, despite the fact that this type of lithology contains a significant amount of world's oil reserves.

Polymer flood gas has been proven to be the most effective EOR method for sandstone reservoirs. However, application of this technique on carbonates is limited due to unfavorable conditions for the use of polymer (as discussed in Chapter 1). ASG method can be an alternative for polymer flooding in this type of rock, since it combines both concepts of IFT lowering and using foam as mobility control agent. Additionally, some of unfavorable conditions for polymer are likely favorable for foam.

A systematic and experimental study of ASG on carbonates was performed and presented in this chapter for better understanding and further investigation on applicability of this process. The chapter is outlined with detailed description of materials, experiment set-up and procedure. Later, discussion of experimental results is carried out to evaluate the performance of ASG process, as well as its applicability.

4.2 MATERIALS

4.2.1 Chemicals, Fluids and Rock

4.2.1.1 Surfactants

Two primary surfactants, Sasol TDA-(PO)13-sulfate (S8D) and Exxal TDA-(PO)13-sulfate (S13D) were used. Each of was mixed with co-surfactant C_{15-18} IOS (S2 , internal olefin sulfonate) at different ratios to form 2 formulae which gave best results for phase behavior. Details of surfactants are given below.

Table 4.1 – Surfactant Details

Surfactant	Activity (%wt)
Sasol TDA-(PO)13-sulfate (S8D)	83.68 %
Exxal TDA-(PO)13-sulfate (S13D)	84.40 %
C_{15-18} IOS (S2)	22.38 %

4.2.1.2 Formation Brine and Crude Oil

Formation Brine

One synthetic brine was made based on formation fluid analysis to represent the actual fluid in the reservoirs. Total dissolved solids (TDS) concentration of the brine is 9366 mg/liter. Brine composition is given below.

Table 4.2 – Brine Composition

Ion	Concentration (mg/liter)
Ca^{++}	281
Mg^{++}	219
Na^{+}	2660
Cl^{-}	3799

Crude Oil

Yates oil was used. This crude oil has viscosity of 17 cP and belongs to a fractured carbonate reservoir located in southern Pecos County, west Texas. This reservoir is now very mature after a long time of being produced (from 1920s), and a

good candidate for chemical EOR. Before using, crude oil was filtered through a 0.45 μm filter paper to remove large particles that could cause plugging.

4.2.1.3 Core Sample

A carbonate rock named Pink Limestone Desert was used. This rock has average porosity of 285 to 30%, and permeability (to air) of 95 md to 120 md. For experiment, core slabs were drilled to obtain core samples about 11.5 inches in length and 1.5 inches in diameter.

4.2.2 Equipments

4.2.2.1 Core Holder

Core holder manufactured by Phoenix Instruments Inc., is used for all of experiments. Core holder is designed so that a core sample of 12 inch long and 1.5 inch in diameter can fit in. There are three pressure taps along the body of core holder, located at 4, 8 and 12 inches from the bottom and connected to pressure transducers for pressure recording. A rubber sleeve lines inside core holder to separate core sample from mineral oil, which is injected to the annular space between core holder and rubber sleeve to create confining pressure. Confining pressure is always 400 – 500 psi higher than pressure in core sample to prevent injected fluids from leaking along the core sample, ensuring the accuracy of mass balance. Core holder is placed vertically and injection of al fluids starts from the bottom.

4.2.2.2 Liquid Pump

ISCO LC-5000 liquid pump was used. The pump inlet is connected to mineral oil source to refill the piston column, and the outlet ties to the container of injected liquids. Mineral oil acts as displacing fluid to inject desired liquids in container to the core holder.

4.2.2.3 Gas Flow Controller

Gas flow controller from Brooks (model: SLA 5850) was used for the purpose of controlling the gas injection rate.

In order to have the best performance, upstream and downstream of the controller were maintain at 600 and 550 psi, respectively, which are the calibrated pressures and also the conditions to have the most accurate gas flow rate from the controller.

4.2.2.4 Back Pressure Regulator (BPR)

The concept of BPR is to create a constant pressure at the upstream of BPR and prevent the fluids from flowing through it until a higher pressure at the upstream is reached. Another advantage of using BPR is to lower the effect of gas expansion at the outlet of core holder.

For coreflood experiments, BPR was connected at the outlet of core holder to create a constant pressure of 480 psi, which is also the actual reservoir pressure taken in this study.

4.2.2.5 Transducers

This device records pressures along the core sample throughout the experiments. Two types of transducers were used: absolute and differential transducers. Absolute transducer measures the actual pressure at a certain location on the core, whereas the differential one measures the pressure drop between to locations. For high pressure experiments, transducers were calibrated to have the range from 0 – 4000 psi. For experiments at atmospheric pressure, the range was re-calibrated to 0 – 20 psi.

4.3 EXPERIMENT PROCEDURE

4.3.1 Phase Behavior Procedure

4.3.1.1 Aqueous Stability Test

This test is to investigate the solubility as well as stability of surfactant mixture in electrolyte solution, at different salinities encountered during corefloods and phase behavior. First, concentrated stock solutions of surfactants are mixed with brine in pipettes. Each pipette is then added with different amounts of sodium chloride solution to vary salinity. All pipettes are then let to settle for at least one hour. The chemical solution is considered stable if there are no visible signs of cloudiness, precipitation or phase separation. And the salinity for which the chemical solution starts having any of those signs above is called critical salinity tolerance. It is recommended that a chemical solution should never be injected at salinity above its critical salinity tolerance.

4.3.1.2 Phase Behavior Screening

Phase behavior screening is the most important step in a chemical EOR process. Other activities can not be proceeded if a good phase behavior, which economically and effectively fits all bound conditions of a particular EOR project, has not been confirmed.

Phase behavior includes mixing of aqueous surfactant solution, saline water (or sodium chloride solution), alkali (if needed) and crude oil into a series of pipettes. Salinity is different in each pipettes by changing the amount of saline water (or sodium chloride solution) added into it. This series of pipettes serves as an indication of salinity range for Type I, Type III and Type II microemulsions.

4.3.1.3 Foaming Test

This test provides a preliminary and quick evaluation on foaming ability of surfactants. On the other hand, to check whether or not surfactants can form stable foams. Foaming test is very simple to conduct. First, surfactant solutions are dispensed into a series of pipettes. Each pipette has is then added different amount of sodium chloride solution to create salinity gradient of interest. Second, all pipettes are

placed into centrifuge machine for one minutes. This step results in the formation of bulk foam column on top of liquid phase. Third, variation in height of foam column is recorded with time. The amount of time in which foam column remains half of the original is an indication of foaming ability. Surfactant that has the best foaming ability will have longest time for foam destruction.

4.3.2 Coreflood Procedure

4.3.2.1 Coreflood set-up

All of equipments described in section 3.2.2 are assembled to form a coreflood set-up as seen in figure 3.1 below. In addition, the core holder is placed inside a convection oven under 30^0C degree, which is the real temperature of the reservoir. This step is to keep crude oil properties unchanged and coreflood is performed under conditions similar to that of reservoir.

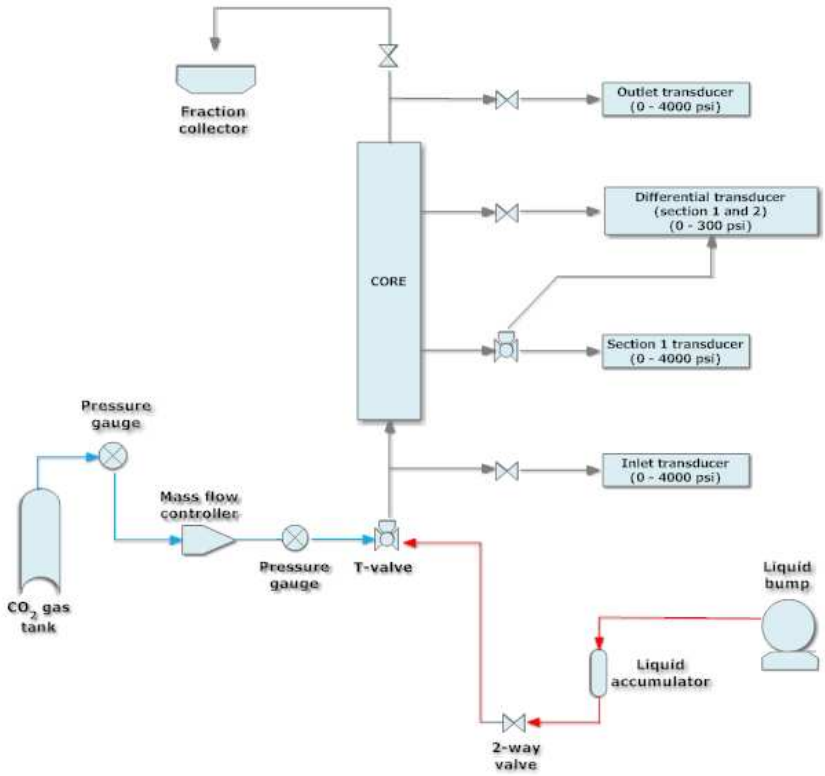

Figure 4.1 – Schematic of experiment set-up

4.3.2.2 Coreflood Procedure

Core Sample Preparation

Core samples are drilled from slabs to have a length of 11.5 inches and diameter of 1.5 inches. Cores are then washed with de-ionized and placed in convection oven under 120^0C degree to dry out for 2 days. Before putting in core holder, cores are wrapped around with silver foil, followed by another shrinking plastic layer. The foil prevents CO_2 from coming into contact with rubber sleeve since CO_2 can damage rubber materials by diffusing into them. Two ends of core are covered by caps which have half-inch diameter hole at the center and concentric groves etched on one side (in contact with the core). The concentric groves ensure a uniform distribution of injected fluid on the surface of the core ends.

The wrapped core is then loaded into core holder. Three holes are drilled on the core based on positions of pressure taps to create pressure communication between the core and transducers. Then confining pressure is applied to core holder by injecting mechanical oil and maintained at 350 – 400 psi higher than pressure the core is going to be conducted on. All flow tubings are connected and system is then checked for leaks. If there is no leak, the system is vacuumed for 4 -6 hours to remove all air inside. Once vacuuming is done, the core is ready for fluid injection. In ASG process, injection of fluid starts from the bottom of core holder and follows the order of: (1) brine saturation; (2) oil saturation; (3) water flood; (4) chemical slug and drive injections.

Brine Saturation

Synthetic brine with compositions similar to reservoir brine is injected to the core for several pore volumes until steady pressure drop along the core is obtained. Main purposes of this step are listed below:

- Determine pore volume and porosity of the core by using mass balance method. These parameters will be used to design following steps. The core is injected at a fixed rate while recording pressure drop along the core and collecting fluid at effluent. Once pressure drop is steady and the rate at

effluent is equal to that at the inlet, indicating the core is fully saturated, pore volume and porosity are calculated as:

$$\text{Pore volume (PV)} = \frac{M_{injected} - M_{produced}}{\rho_{brine}}$$

$$\sigma = \frac{\text{PV}}{V_{bulk}} = \frac{\text{PV}}{\pi \text{D}^2 L / 4}$$

where: $M_{injected}$ = amount of brine injected into the core (grams)

$M_{produced}$ = amount of brine collected at effluent (grams)

ρ_{brine} = density of brine (grams/cm^3)

D = core diameter (cm)

L = core length (cm)

- Determine absolute permeability (to brine) of the core by injecting at different rates and recording steady pressure of each rate. Absolute permeability is then calculated through Darcy's law. If performed properly, the plot of steady pressure versus rate should be a straight line.

$$k_{abs} = \frac{Q\mu_{brine}L}{A\Delta P} = \frac{Q\mu_{brine}L}{\pi \text{D}^2 / 4 \ \Delta P}$$

where: k_{abs} = absolute permeability (milidarcy, md)

Q = rate (cm^3/hr)

μ_{brine} = brine viscosity (cP)

ΔP = steady pressure along the core (psi)

Oil Saturation

This step models the reservoir when it has been produced yet. Crude oil is injected into the core at a fixed rate until 100% oil cut is obtained at the effluent and steady pressure drop occurs. Initial oil saturation is calculated by using mass balance

while oil effective permeability is computed through Darcy's law. End – point oil relative permeability is the ratio of oil effective permeability and absolute permeability (to brine).

$$S_o = \frac{V_{injected} - V_{produced}}{\text{PV}} \times 100$$

$$k_o = \frac{Q_o \mu_o L}{\pi \text{D}^2 / 4 \ \Delta P}$$

$$k_{ro} = \frac{k_o}{k_{abs}}$$

where: $V_{injected}$ = volume of oil injected into the core (cm^3)

$V_{produced}$ = volume of oil collected at effluent (cm^3)

PV = pore volume (cm^3)

Q_o = oil rate (cm^3/hr)

S_o = initial oil saturation (%)

μ_o = oil viscosity (cP)

k_o = effective oil permeability (md)

k_{ro} = end – point oil relative permeability (md)

Water Flood

Water flood uses exactly the same brine as in *brine saturation* step to displace oil in the core. However, the rate is kept unchanged till the end of this step. Brine is injected at an interstitial velocity of 2ft/day until 100% water cut is obtained at effluent and pressure drop is steady. Residual oil saturation, water effective permeability and end – point water relative permeability are calculated in this step.

$$S_{ro} = \frac{V_o - V_{produced}}{\text{PV}} \times 100 = \frac{\left(S_o \times \text{PV}\right) - V_{produced}}{\text{PV}} \times 100 = \left(S_o - \frac{V_{produced}}{\text{PV}} \right) \times 100$$

$$k_w = \frac{Q_w \mu_{brine} L}{\pi \text{D}^2 / 4 \ \Delta P}$$

$$k_{rw} = \frac{k_w}{k_{abs}}$$

where: V_o = initial volume of oil in the core (cm^3)

$V_{produced}$ = volume of oil produced at effluent (cm^3)

PV = pore volume (cm^3)

Q_w = brine rate (cm^3/hr)

S_{ro} = residual oil saturation (%)

μ_{brine} = brine viscosity (cP)

k_w = effective water permeability (md)

k_{rw} = end – point water relative permeability (md)

Slug and Drive Injections

A surfactant slug of 0.3 PV is co-injected (or alternately injected) with CO_2 into the core. Salinity of slug solution is the optimum salinity that was determined from phase behavior. Upon the completion of slug injection, a drive solution with lesser concentration of surfactant is co-injected (or alternately injected) with CO_2 until no more oil and microemulsion is seen at the effluent. Fluids collected at the effluent are used to calculate oil recovery and to analyze salinity gradient, pH, surfactant concentrations.

4.4 RESULTS AND DISCUSSION

4.4.1 Phase Behavior Results

The objective was to find a surfactant formula that gives optimum salinity close to that of formation brine (~ 10000 ppm) and no alkali is required. More than 25 formulae have been tested for phase behavior with Yates crude oil, and only two of them showed good results and best fitted the above conditions. Details are given in table 4.3 and 4.4.

Table 4.3 – Surfactant Formula

Formula	Surfactant	Concentration (%wt)	Used in coreflood
A	Exxal TDA-(PO)13-sulfate	0.8%	ASG 1
	C_{15-18} IOS	0.05%	ASG 2
B	Sasol TDA-(PO)13-sulfate	0.9%	ASG 3
	C_{15-18} IOS	0.1%	ASG4

Table 4.4 – Phase Behavior Results

Formula	Optimum salinity (TDS, ppm)	Solubilization ratio (cm^3/cm^3)	Aqueous stability limit (TDS, ppm)	Type III window (TDS, ppm)
A	12000	20	30000	10000 – 14000
B	14000	18	28000	9000 – 18000

Formula A is a combination of Exxal TDA-(PO)13-sulfate and C_{15-18} IOS with ratio of 16:1, respectively. Exxal TDA-(PO)13-sulfate is very hydrophobic due to a large number of PO group added into it and is suitable for low salinity application. However, this surfactant has very low salinity tolerance. Thus, a very small concentration of C_{15-18} IOS was added to increase the stability of surfactant mixture in aqueous phase. Optimum salinity was around 12000 ppm and solubilization ratio was found to be 20.

Sasol TDA-(PO)13-sulfate is very similar to Exxal TDA-(PO)13-sulfate with almost the same properties. The only difference is that Exxal TDA-(PO)13-sulfate has longer carbon chain. Combination Sasol TDA-(PO)13-sulfate and C_{15-18} IOS in formula B gives optimum salinity of 14000 ppm and solubilization ratio of 18. Optimum salinity is higher than formation brine (~ 10000 pp). However, formation brine salinity is covered within Type III window of this formula (9000 – 18000 ppm). Additionally, as seen from figure 4.4, the last tube represents TDS of 10000 ppm and has very thick microemulsion phase, indicating very low IFT and good solubilization.

As seen from table 4.4, two formulae have relatively close solubilization ratios. By using Chun-Huh model, IFT was estimated to be ~ 10^{-3} dynes/cm. which is a typical value required for reduction of residual oil saturation S_{or}. Moreover, both formulae offer a wide range of Type III microemulsion, which is good when take into account the salinity contrast in real reservoir.

Below are pictures and charts of phase behaviors and solubilization ratios for two formulae.

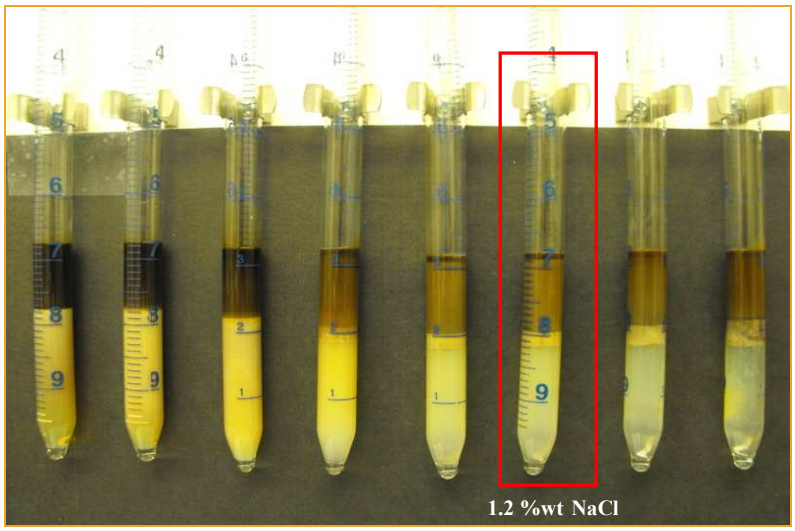

Figure 4.2 – Phase behavior of formula A

From left to right, NaCl concentration varies from 0.6 %wt to 1 %wt (0.1 %wt increments) for the first 5 pipettes. The last 3 pipettes start with 1.2 %wt to 1.6 %wt (0.2 %wt increments). Pipette with optimum salinity is covered in red rectangular

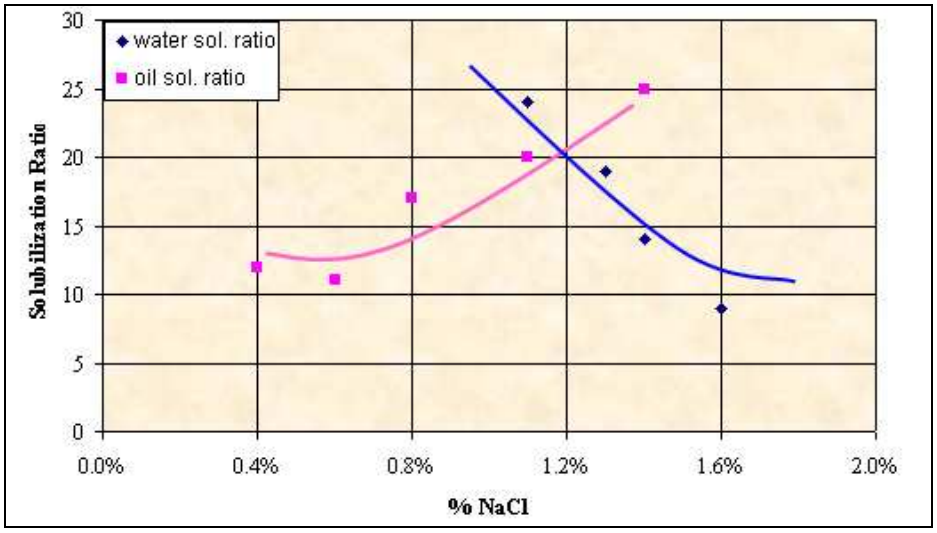

Figure 4.3 – Solubilization ratio versus NaCl concentration for formula A

Figure 4.4 – Phase behavior of formula B

NaCl concentration varies from 0.1 %wt to 1% wt from left to right (0.1% increments)

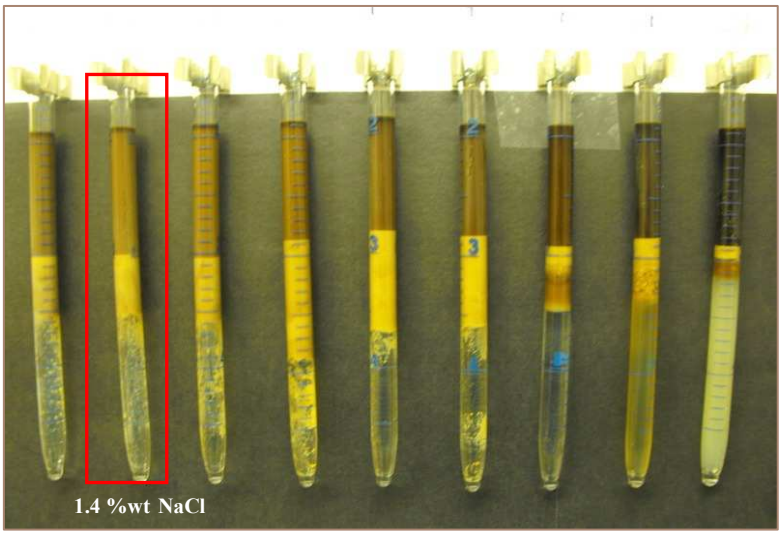

Figure 4.5 – Phase behavior of formula B (continue)

NaCl concentration varies from 1.2 %wt to 2.8 %wt from left to right (0.2 %wt increments). Pipette with optimum salinity is covered in red rectangular

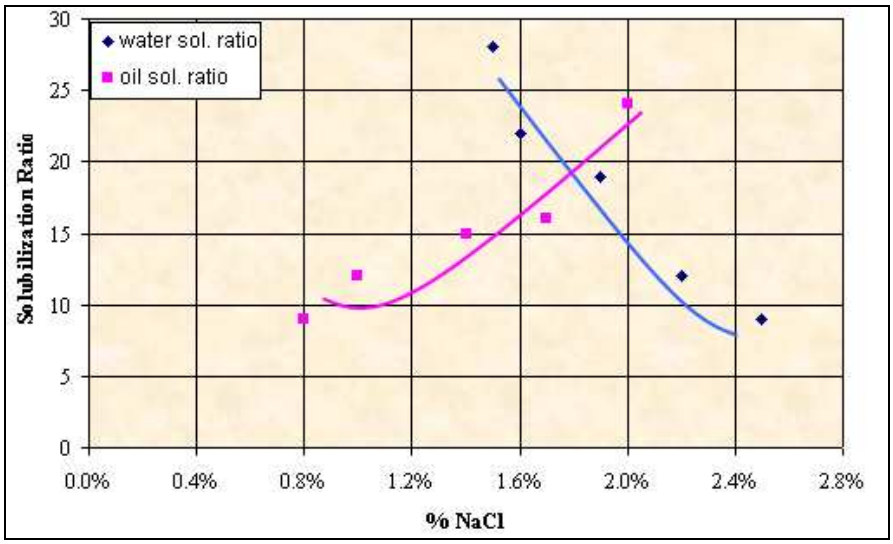

Figure 4.6 – Solubilization ratio versus NaCl concentration for formula B

4.4.2 Coreflood Results

4.4.2.1 Coreflood Summary

Four ASG corefloods were carried out on Pink limestone rocks with a back pressure of 480 psi. The first two corefloods, ASG 1 and ASG 2, were performed with formula A, while formula B was used for ASG 3 and ASG 4 (refer to table 4.3 for details on surfactant formula). Below is the summary of all four corefloods. To avoid confusion, the term PV (pore volume) is only used to indicate the volume of injected liquid.

ASG 1 was conducted to evaluate the foaming ability of surfactant formula. There was no oil saturation in this case. After brine saturation, core was injected with only slug solution. Next, it was washed with brine to remove all surfactant and then co-injected with gas and slug at 35% quality. Pressure drop with gas and no gas injection were compared for foam generation.

ASG 2 followed the standard procedure as presented in section 4.3.2.2. However, there was no gas injection during slug and drive floodings. Results of this coreflood are compared with ASG 3 where foam is generated for mobility control.

ASG 3 and ASG 4 followed standard procedure as described in section 4.3.2.2. Specifically, slug and drive were con-injected with gas at 50% (1ft/day for both gas and liquid) in *ASG 3*. In contrast, surfactant – alternating – gas (SAG) was used in *ASG 4*, where each cycle contains 0.1 PV of slug and 0.15 PV of gas.

Table 4.5 – Experiment Details

	ASG 1	ASG 2	ASG 3	ASG 4
Porosity (%)	29	31	31	30
Permeability (to brine, md)	118	105	100	92
Liquid rate for slug and drive (ft/day)	2	2	1.1	2
Gas rate for slug and drive (ft/day)	1.1		1	1
Foam quality (%)	35		45	
Liquid and gas slug for SAG (each cycle)				0.15 PV gas 0.1 PV liquid
Surfactant concentration in slug	0.8 % S13D 0.05% S2	0.8 % S13D 0.05% S2	0.9 %S8D 0.1% S2	0.9 % S8D 0.1% S2
Slug salinity (ppm)	10,000	10,000	10,000	10,000
Surfactant concentration in drive	0.1 % S2	0.1 % S2	0.1 % S2	0.1 % S2
Drive salinity (ppm)	4000	4000	4000	4000

Table 4.6 – Main Results of Coreflood

	ASG 1	ASG 2	ASG 3	ASG 4
Residual oil saturation (%) (ROIP)		29	27	29
Oil recovery (% of ROIP)		44	61	55
Oil recovery (% of OOIP)		16	21	20

4.4.2.2 Results and Discussion

ASG 1

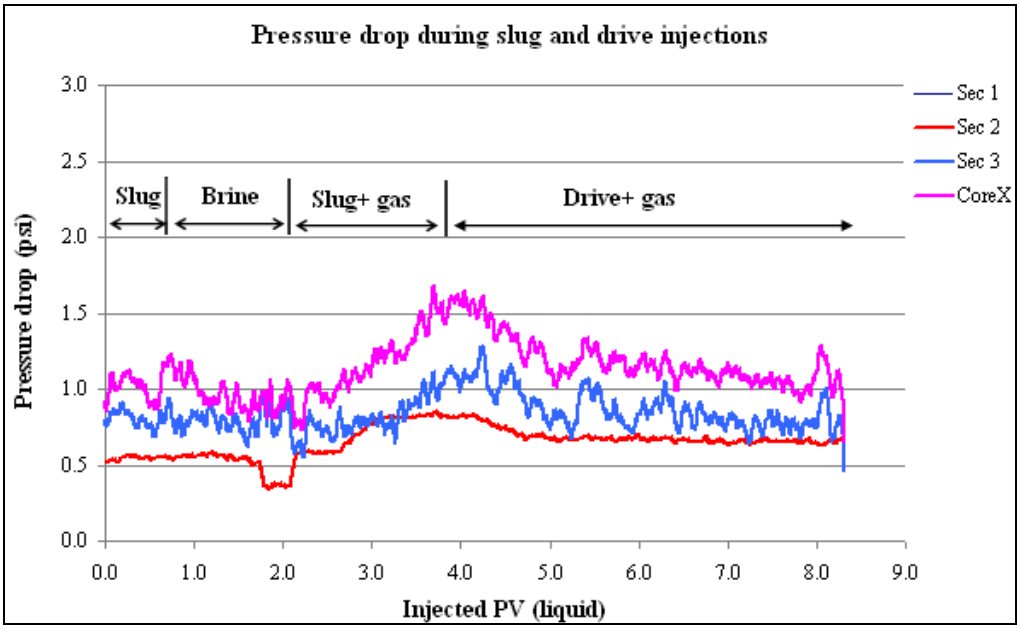

Figure 4.7 – Pressure drop during chemical injection of ASG 1

Figure 4.5 shows pressure data for ASG 1. Notations in black color on top of the curves indicate type of injection and pore volume taken by that injection type. As seen from the figure, slug solution was injected ~ 0.5 PV, followed by a 1.5 PV brine injection. Pressure drops in both cases are relatively equal, around 1 psi.

Pressure in each section started going up upon the co-injection of slug and gas. First, pressure in section 2 (red line) goes up at 2.5 PV while pressure in section 3 (blue line) remains the same. At 3.2 PV, pressure in section 2 levels off and that of section 3 starts increasing. This observation indicates the formation of foam in section 2 and its propagation to section 3. At the end of co-injection, pressure drop is 1.5 psi, which is higher than that when no gas was injected. The difference of 0.5 psi is another proof of foam formation.

During the co-injection of gas and drive solution, pressure drops in all section go down and level off at the same pressure drop of no gas-injection case, suggesting that either there is no foam or very weak foam is created during the drive flooding.

ASG 2

After water flooding, a slug of 0.3 PV is injected at 2ft/day (the same rate as in water flood). Pressure drop profile is shown in figure 4.6.

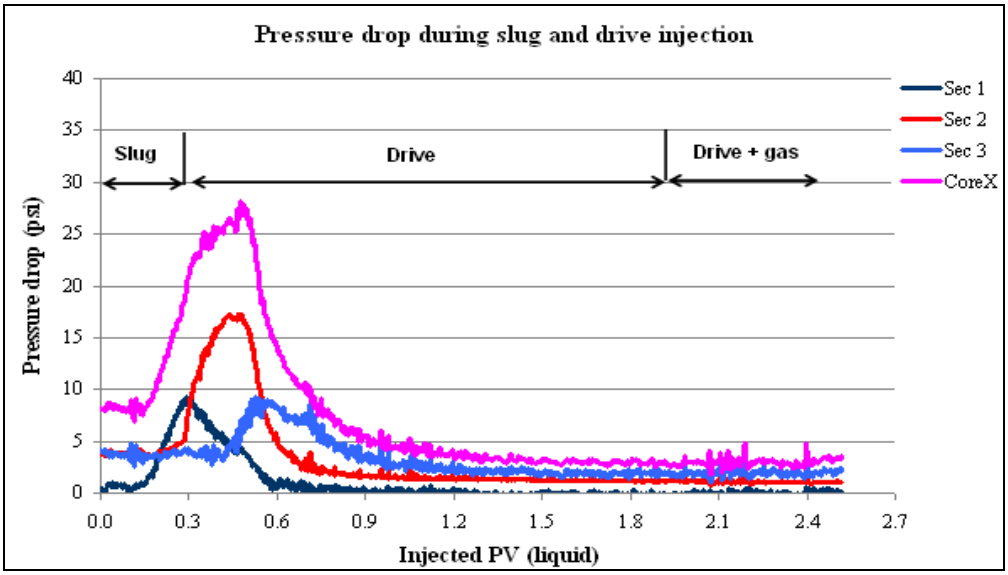

Figure 4.8 – Pressure drop during chemical injection of ASG 2

The increasing trend in pressure drop during slug injection indicates the formation of oil bank at the displacement front of microemulsion. Moreover, pressure

drop increases orderly starting from section 1 presents the propagation of oil bank in those sections. At the end of slug injection, pressure drop in section 1 levels off whereas that of section 2 reaches its peak, suggesting that microemulsion and oil bank initially formed in section 1 have been transported to section 2.

The same phenomenon happens at the beginning of drive where pressure drop in section 2 starts to decrease and section 3 begins increasing. At this point, microemulsion and oil have travelled to section 3 and been being produced. After 0.6 PV, all pressures start to level off, indicating a decrease in viscous phase saturation as oil is being produced. This leads to the increase in oil recovery curve in figure 4.7, starting from 0.6 PV.

As seen from figure 4.6, during slug injection, section 1 has an increase of 7 psi (from 1 to 8 psi) whereas that of section 2 is almost doubled, 13 psi. That observation when put together with the fact that permeabilities of section 1 and section 2 are very close (122 md and 108), the length is equal, injection rate is kept the same throughout experiment, will suggest that all of microemulsion and oil bank caused a 7 psi pressure drop in section 1 were pushed into section 2. The same concept applied to section 3. However, with only 5 psi increased, it is reasonable to say that a significant amount of microemulsion was trapped in section 2, which accounts for low oil recovery. This argument matches with the fact that there was no microemulsion produced during the experiment.

Trapping of microemulsion can be explained by the formation of viscous microemulsion and poor sweep efficiency due to the absence of foam as mobility control agent. At the end of water flooding, pressure drop across the core at 100% water cut was 10 psi. During slug injection, a 25 psi drop across the core (pink line) was observed. Since water flood and slug are injected at the same rate and a lower IFT will occur when slug contacts with oil due to the presence of surfactant, pressure drop is expected to be less or equal, for maximum, to that at the end of water flood, given the absence of foam. Therefore, the excessive 15 psi must participate in the formation of a very viscous phase, which is more likely microemulsion. Moreover, residual oil is resides pushed into less permeable regions after water flood. Viscous microemulsions are formed in those regions when surfactant comes into contact with

oil. Drive solution is injected at Type I to transport microemulsion and surfactant back to aqueous phase based on the concept of salinity gradient (figure 4.8). However, viscosity contrast and the lack of mobility control agent let drive solution flow in higher permeability regions, leaving behind a significant amount of trapped microemulsion.

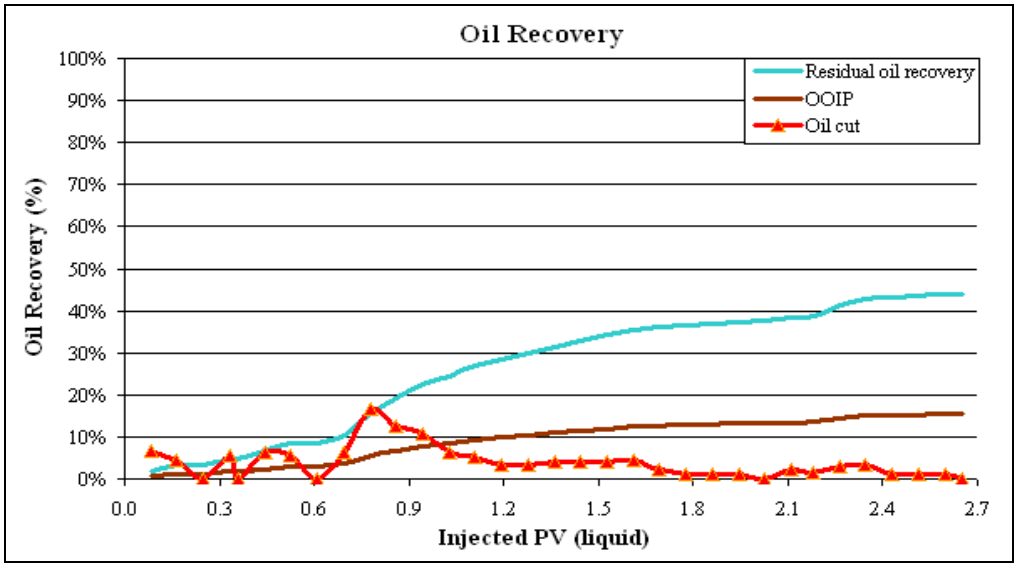

Figure 4.9 – Oil recovery for ASG 2

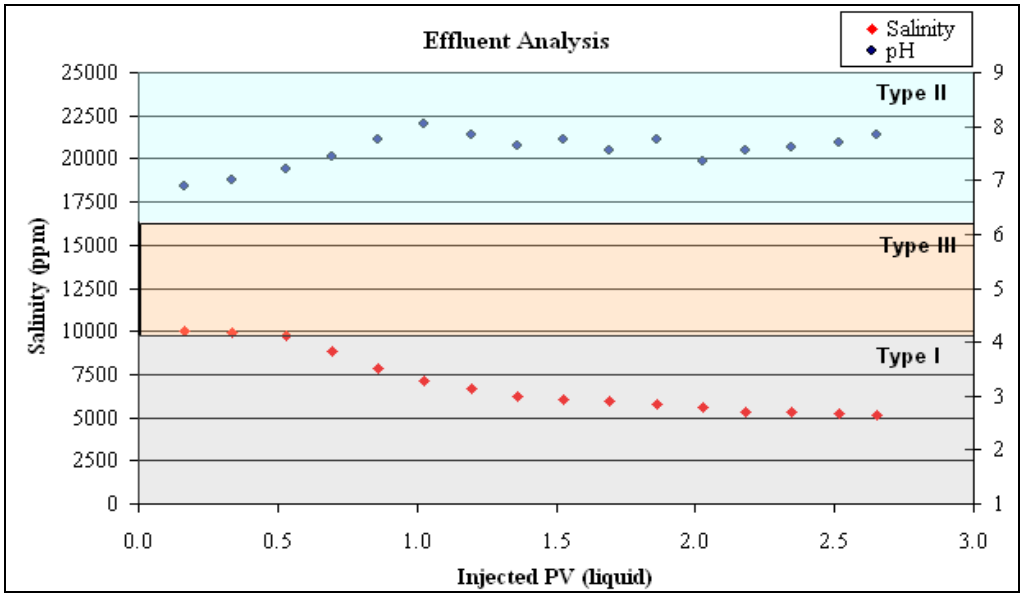

Figure 4.10 – Effluent salinity and pH

ASG 3

As seen from figure 4.9, pressure drop in section 1 goes up to very value with the co-injection of gas and liquid. In contrast, pressure drop reduces when only liquid flooded. Starting from 0.15 PV to the end of slug flooding, only liquid is injected. Pressure in section 2 experiences an increase then levels off, together with section 1 while section 3 is almost constant.

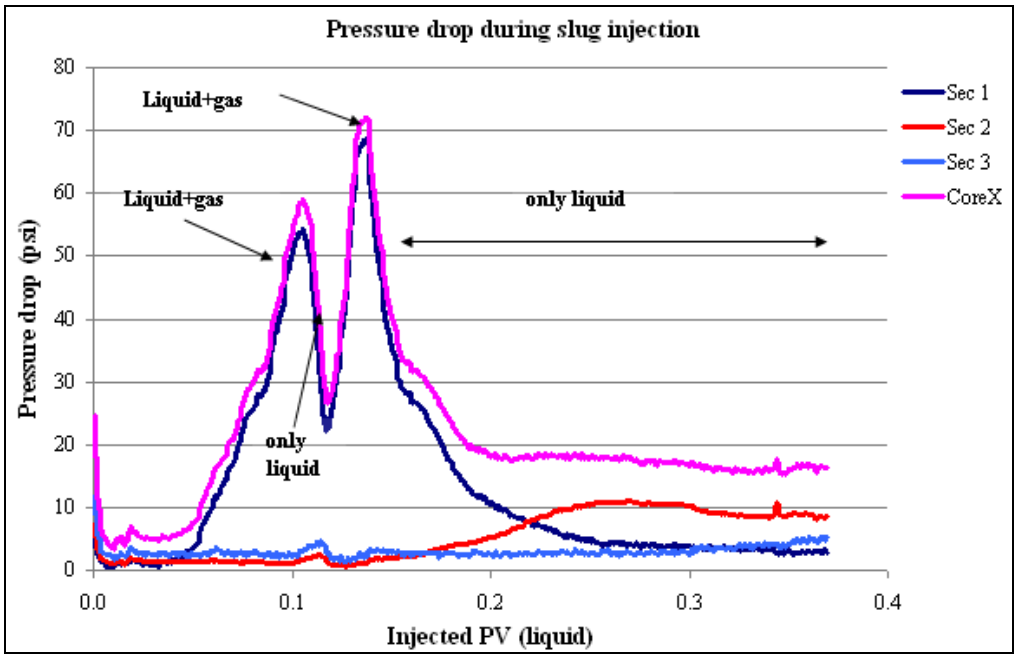

Figure 4.11 – Pressure profile during slug injection of ASG 3

The same situation happened to drive injection (figure 4.10). The formation and trapping of viscous microemulsion in low permeability regions together with formation of oil bank at the displacement front of microemulsion phase, which was proposed in ASG 2, can be used to explain this phenomenon. Moreover, in the presence of foam to increase the sweep efficiency, more surfactant is diverted into contact with residual oil and, therefore, more viscous microemulsion is formed, resulting in higher pressure drop compared to ASG 2.

Formation of immobilized microemulsions and foam result in gas trapping since foam reduces apparent viscosity of gas and immobilized microemulsions block

the flow path. However, liquid can flow through thin film liquid separating foams (lamella) and thus, pressure drop is decreased when only liquid flows.

Above 0.6 PV pressure drop across the core levels off even with the co-injection of gas and liquid. This is due to the oil bank breakthrough at 0.45 PV, and until 0.6 PV, most of oil in oil bank has been produced, corresponding the gradually increase of oil recovery curve (figure 4.11). Microemulsion breakthroughs at 0.75 PV where oil recovery is almost at its peak.

This experiment has the highest recovery, but most of oil is recovered through highest pressure drop period during the injection. Therefore, it is not true to say this is a successful coreflood. However, by using the hypothesis as stated above, we can clearly see the effect of foam for mobility control.

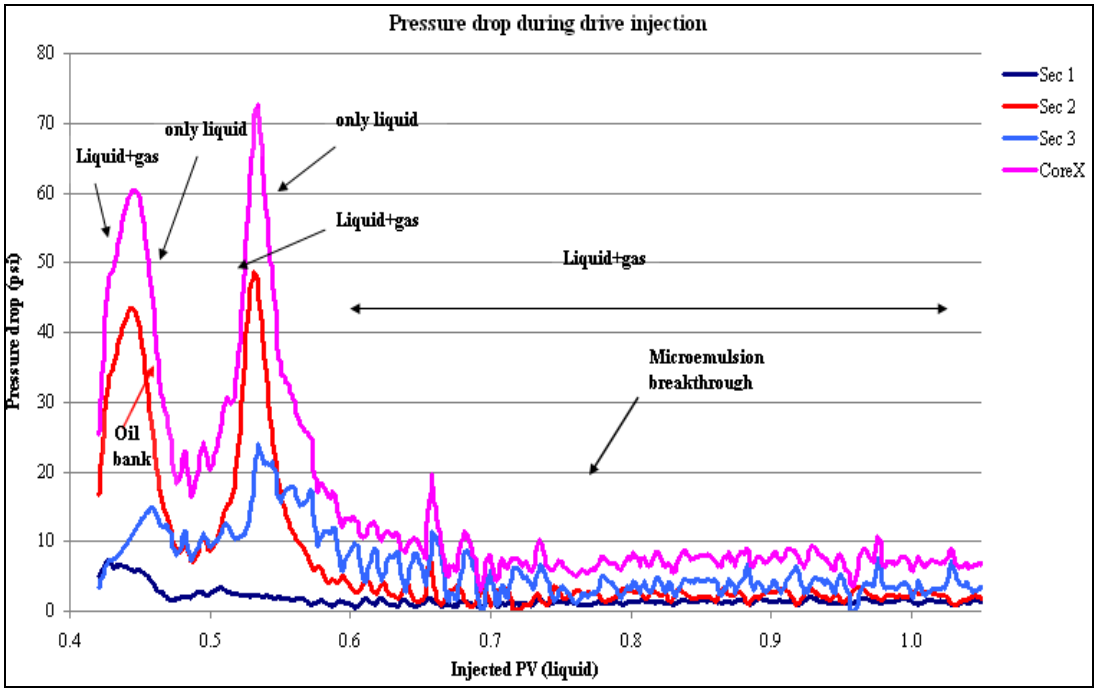

Figure 4.12 – pressure drop profile during drive injection

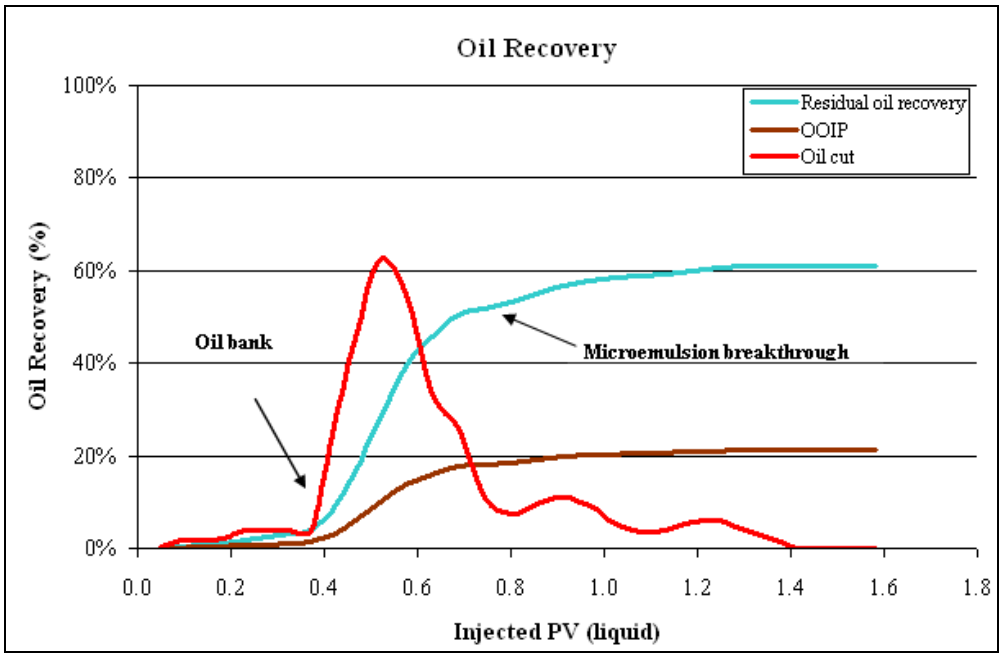

Figure 4.13 – Oil recovery in ASG 3

ASG 4

Chemical flooding in this coreflood was done with Surfactant – Alternating – Gas (SAG). One cycle contains the injection of 0.15 PV of liquid and 0.1 PV of gas.

In this case, pressure drop changes in a complete opposite way to ASG 3, that is, it increases during the liquid slug and decreases with gas slug. Pressure drop in each liquid slug is reduced corresponding to a certain amount of oil being produced (figure 4.13). This results in the slowly increase in oil recovery curve (figure 4.14).

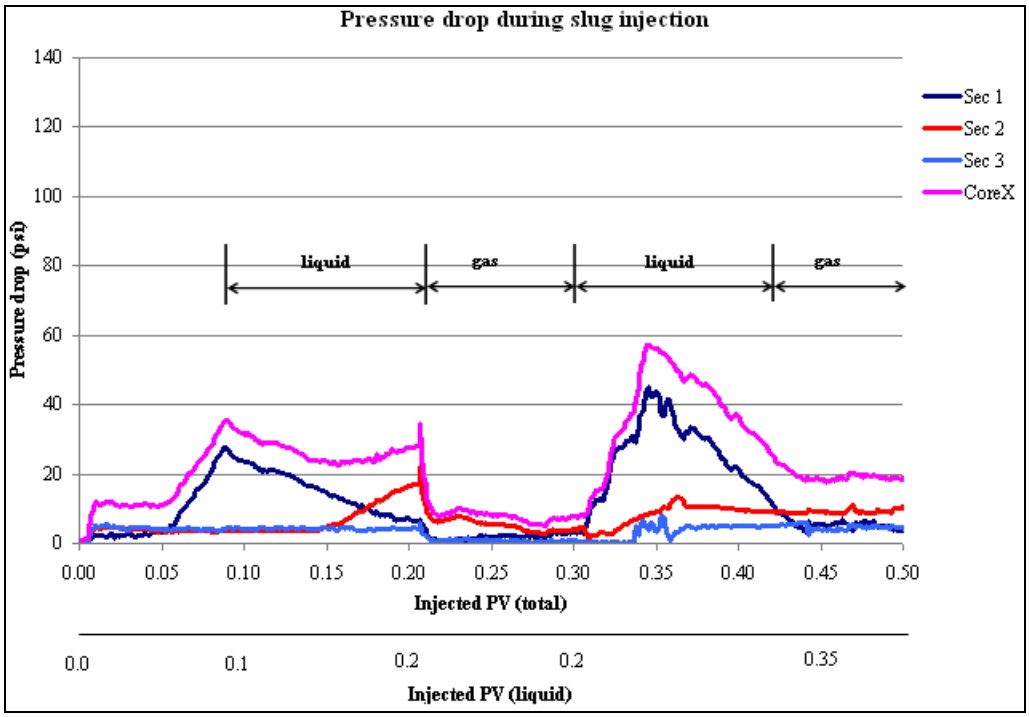

Figure 4.14 – Pressure drop profile during slug injection of ASG 4

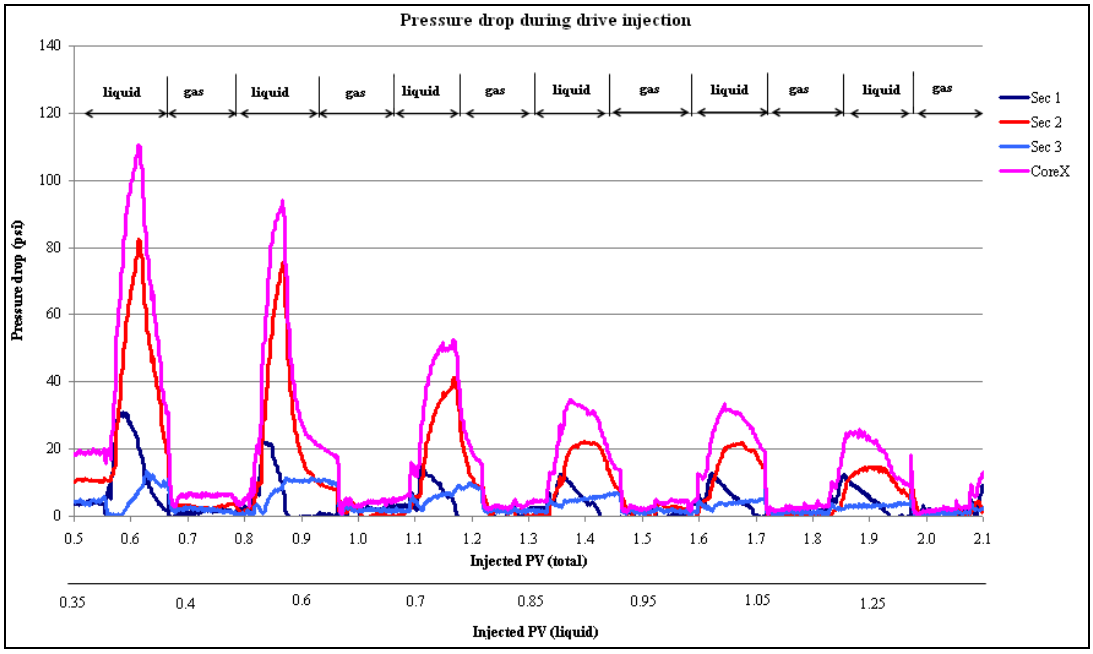

Figure 4.15 – Pressure drop profile during drive injection of ASG 4

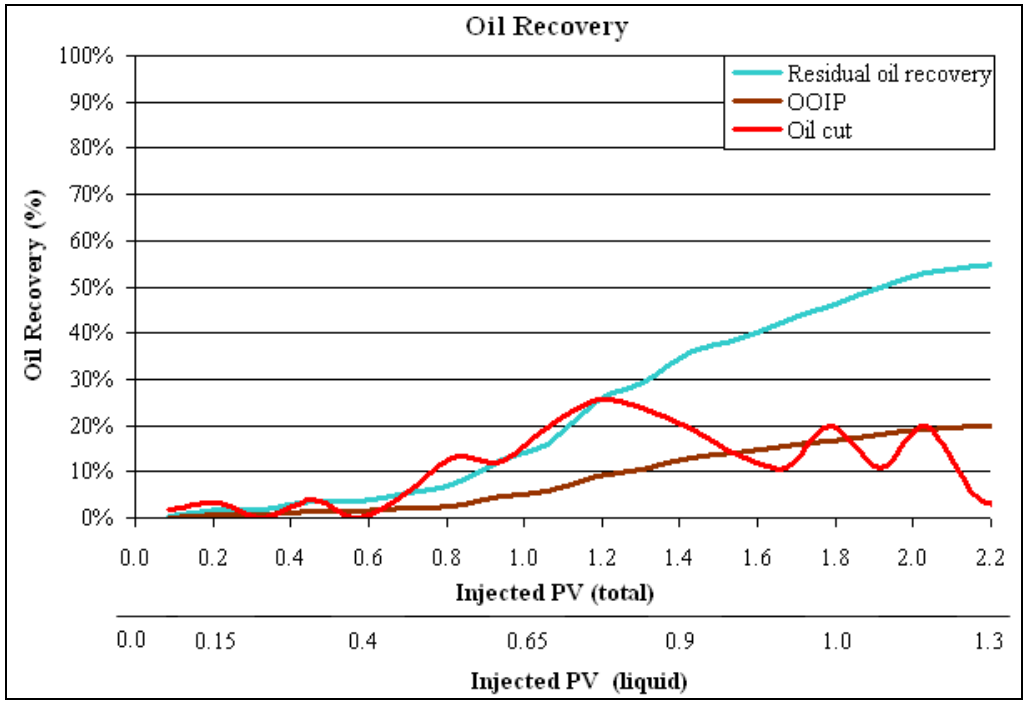

Figure 4.16 – Oil recovery in ASG 4

4.4.3 Chapter Summary

The series of coreflood provided a good understanding about ASG process. Foam formation and performance were observed. Although there were some other factors involved but the contribution of foam to mobility control was significant.

Two formulae designed for Yates crude oil showed good phase behavior and provided low IFT. The recoveries in corefloods were acceptable. However, the author would not recommend the use of these formula since extremely high pressure was obtained, which can be performed in the real field due to limits on system capacity.

Within the conditions in which this experiment series was conducted, we can conclude that co-injection of gas and liquid is more effective than SAG, since it yields lower pressure drop and faster recovery.

CHAPTER 5

CONCLUSIONS AND RECOMMENDATIONS

5.1 Conclusion

The twin-tailed dioctylglycerine surfactants showed a very good performance compared to conventional surfactants. Even above the cloud point of the surfactants, the twin tailed surfactant (DOG-9) creates a significant mobility reduction, likely due to favorable partitioning into the CO_2 phase.

Basic understanding of ASG process was presented in chapter 4. Even though there were some unfavorable results but the role of foam as mobility control agent was clearly showed. The recoveries from core floods were remarkable, highlighting the potential of ASG as a new EOR technique.

Surfactants used for phase behavior showed good results and low IFT. However, the possibility for these surfactants to form viscous microemulsion is positive. Therefore, the use of these surfactants is not recommended. Optimization needs to be performed on designing surfactant formula in order to have a good phase behavior.

5.2 Recommendations

Based on the results obtained from this study, the author would like to recommend the future works on ASG as:

- A full and systematic study about factors affecting ASG needs to be investigated in order to better understand and apply the process for field project.
- Foam stability in different microemulsion environments must be studied since foam stability is main key to the success of ASG.
- Determine which injection strategy is the best for ASG method, co-injection or Surfactant – alternating – gas (SAG).

REFERENCES

1. E. Manrique, C. Thomas, and R. Ravikiran: “EOR: Current Status and Opertunities”, SPE 130113, 2010.
2. G. J. Hirasaki and H. R. van Domselaar: “Evaluation of The Salinity Gradient Concept”, AIME, 1983.
3. W. R. Rossen: “Theories of Foam Mobilization Pressure Gradient”, SPE/DOE 17358, 1988.
4. J. E. Hanssen and M. Dalland: “Foams for Effective Gas Blockage in the Presence of Crude Oil”, SPE/DOE 1990.
5. S. I. Chu: “Conditions for Generating Foam in Porous Media”, SPE 22628.
6. Daan Veeningen and Pacelli L. J. Zitha: “Understanding Foam Flow Physics: The Role of Permeability”, SPE 38197.
7. R. N. Heal and R. L. Reed: “Multiphase Microemulsion Systems”, SPE 5565.
8. P. A. Gauglitz and F. Friedmann: “Foam Generation in Porous Media”, 2002.
9. D. A. Hudgins and T. H. Chung: “Long – Distance Propagation of Foams”, SPE/DOE, 1990.
10. F. E. Suffridge, K. T. Raterman and G. C. Russell: “Foam Performance under Reservoir Conditions”, SPE 19691.
11. Feliciano M. Llave and David K. Olsen: “Used of Mixed Surfactants to Generate Foams for Mobility Control in Chemical Flooding”, SPE Reservoir Engineering 1994.
12. Karin Mannhardt and L. L. Schramm: “Comparative Evaluation of Foam Stability to Oil”, SPE 2000.
13. F. Khalil and K. Asghari: “Application of CO_2-Foam as a Means of Reducing Carbon Dioxide Mobility”, JCPT, Volume 5, No. 5. May 2006.

14. B. M. Lescure and E. L. Claridge: "CO_2 Foam Flooding Performance vs. Rock Wettability", SPE 15445.

15. R. Farajzadeh, A. Andrianov, and P. L. J. Zitha: "Foam Assisted Enhanced Oil Recovery at Miscible and Immiscible Conditions", SPE 126410.

16. A. D. Nikolov, D. T. Wasan and D. A. Edwards: "The Effect of Oil on Foam Stability: Mechanisms and Implications for Oil Displacement by Foam in Porous Media", SPE 15443.

17. Wang D., Liu. C., and Wu. W.: "Novel Surfactants that Attain Ultra-Low Tension between Oil and High Salinity Formation Water without adding Alkali, Salts, Co-Surfactants, Alcohol and Solvents", SPE 127452.

18. Mayank Srivastava and Quoc. P. Nguyen: "Application of Gas for Mobility Control in Chemical EOR in Problematic Carbonates Reservoirs", SPE 129840.

19. L. A. Noll: "The Effect of: Temperature, Salinity, and Alcohol on the Critical Micelle Concentration of Surfactants", SPE 21032.

20. E. J. Manrique, V. E. Muci and M. E. Gurfinkel: "EOR Field Experiences in Carbonate Reservoirs in the United States", SPE 100063.

21. Quoc. P. Nguyen, Alexander V. Alaxandrov, and Pacelli L. Zitha: "Experimental and Modeling Studies on Foam in Porous Media: A Review", SPE 58799.

22. Reid B. Grigg, Jyun-Syung Tsau, and F. David Martin: "Cost Reduction and Injectivity Improvements for CO_2 Foams for Mobility Control", SPE 75178.

23. Y. Liu, R. B. Grigg and R. K. Svec: "CO_2 Foam Behavior: Influence of Temperature, Pressure and Concentration of Surfactants", SPE 94307.

24. W. R. Rossen, K. R. Kibodeaux and J. X. Shi: "Injectivity and Gravity Override in Surfactant-Alternating-Gas Foam Process", SPE 30753.

25. Gouyin Zhang and R. S. Seright: "Conformance and Mobility Control: Foams vs. Polymers", SPE 105907.

26. Viet. Q. Le, Quoc. P. Nguyen and Aaron W. Sanders: "A Novel Foam Concept with CO_2 Dissolved Surfactants". SPE 113370.

27. Robert Feng Li, Wei Yan, Shunhua Liu and George J. Hirasaki: "Foam Mobility Control for Surfactant EOR", SPE 113910.

28. Tanzil D. (2001): "Foam Generation and Propagation in Heterogeneous Porous Media", PhD Dissertation, Rice University, Houston, Texas, USA.

29. Jose Manuel Alvarez Martinez (1998): "Foam-Flow Behavior in Porous Media: Effects of Flow Regime and Porous – Medium Heterogeneity", PhD Dissertation, The University of Texas at Austin, Austin, Texas, USA.

30. Laurier L. Schramm: "Foams: Fundamentals and Applications in the Petroleum Industry", published by American Chemical Society, Washington, DC 1994, 47-107.

31. Pope, G. A and Nelson, R. C.: "A Chemical Flooding Compositional Simulator", SPE J, 18, 339-354.

32. Sorbie, K. S: "Polymer-Improved Oil Recovery"", CRC press Inc. Boca Raton, Florida.

33. Yan W.(2006): "Foam for Mobility Control on Alkaline/Surfactant/ Enhanced Oil Recovery Process", PhD Dissertation, Rice University, Houston, Texas, USA.

34. Quoc P. Nguyen (2004): "Dynamics of Foam in Porous Media", PhD Dissertation, Delft University, Netherlands.

35. L. D .Zhang and G. J. Hirasaki: "Favorable Attributes of Alkali-Surfactant-Polymer Flooding", SPE 99744.

36. W. R. Rossen: "Minimum Pressure Gradient for Foam Flow in Porous Media: Effect of Interactions with Stationary Lamellae", Journal of Colloid and interface Science. 139 (2), 457-468, October.

37. Rossen, W.R. 1996. Foams in Enhanced Oil Recovery." In *Foams: Theory, Measurement, and Applications*, ed. R.K. Prudhomme and S. Khan. New York: Marcel Dekker.

38. Sagisaka, M., Fujii, T., Ozaki, Y., Yoda, S., Takebayashi, Y., Kondo, Y., Yoshino, N., Sakai, H., Abe, M., and Otake, K. 2004. Interfacial Properties of Branch-Tailed Fluorinated Surfactants Yielding a Water/Supercritical CO2 Microemulsion. *Langmuir*. **20**, 2560-2566.

39. Thoen, J.A., Bartelink, C.F., Davis, C.S., Varineau, P.T., and Morley, T.A. 2008. Novel alkyloxy-ethers and alkoxylates thereof. International PCT Int. Appl. WO 2008/134387.

40. Turta, A.T. and Singhal, A.K. 1998. Field Foam Applications in Enhanced Oil Recovery Projects: Screening and Design Aspects. Paper SPE 48895 presented at the SPE International Conference and Exhibition in China held in Beijing, China, 2-6 November. doi: 10.2118/48895-MS

41. Wang, Y., Hong, L., Tapriyal, D., Kim, I.C., Paik, I.-H., Crosthwaite, J.M., Hamilton, A.D., Thies, M.C., Beckman, E.J., Enick, R.M., and Johnson, J.K. 2009. Design and Evaluation of Nonfluorous CO_2-Soluble Oligomers and Polymers. *J. Phys. Chem. B*. **113**: 14971.